Remote Sensing of Environment 192 (2017) 176–197

Contents lists available at ScienceDirect

Remote Sensing of Environment

journal homepage: www.elsevier.com/locate/rse

Review

Advances in using multitemporal night-time lights satellite imagery to detect, estimate, and monitor socioeconomic dynamics

Mia M. Bennett *, Laurence C. Smith

Department of Geography, University of California, Los Angeles, 1255 Bunche Hall Box 951524, Los Angeles, CA 90095, USA

ARTICLE INFO

Article history:
Received 10 March 2016
Received in revised form 29 December 2016
Accepted 8 January 2017
Available online 24 February 2017

Keywords:
Nighttime lights
Day/Night Band
Suomi NPP VIIRS
DMSP-OLS
Urbanization
Population
GDP

ABSTRACT

Since the late 1990s, remotely sensed night-time lights (NTL) satellite imagery has been shown to correlate with socioeconomic parameters including urbanization, economic activity, and population. More recent research demonstrates that multitemporal NTL data can serve as a reliable proxy for change over time in these variables whether they are increasing or decreasing. Time series analysis of NTL data is especially valuable for detecting, estimating, and monitoring socioeconomic dynamics in countries and subnational regions where reliable official statistics may be lacking. Until 2012, multitemporal NTL imagery came primarily from the Defense Meteorological Satellite Program - Operational Linescan System (DMSP-OLS), for which digital imagery is available from 1992 to 2013. In October 2011, the launch of NASA/NOAA's Suomi National Polar-orbiting Partnership satellite, whose Visible Infrared Imaging Radiometer Suite (VIIRS) sensor has a Day/Night Band (DNB) specifically designed for capturing radiance from the Earth at night, marked the start of a new era in NTL data collection and applications. In light of these advances, this paper reviews progress in using multitemporal DMSP-OLS and VIIRS imagery to analyze urbanization, economic, and population dynamics across a range of geographic scales. An overview of data corrections and processing for comparison of multitemporal NTL imagery is provided, followed by a meta-analysis and integrative synthesis of these studies. Figures are included that visualize the capabilities of DMSP-OLS and VIIRS to capture socioeconomic change in the post-Soviet Russian Far East and war-torn Syria, respectively. Finally, future directions for NTL research are suggested, particularly in the areas of determining the fundamental causes of observed light and in leveraging VIIRS' superior sensitivity and spatial and radiometric resolution.

Contents

* Corresponding author.
E-mail address: mbennett8@gmail.com (M.M. Bennett).

http://dx.doi.org/10.1016/j.rse.2017.01.005
0034-4257/

1. Introduction

At night, anthropogenic activities such as the electrical illumination of population centers and gas flaring from Siberian oil fields light up the Earth's surface. These nighttime lights (NTL) can be resolved from space by satellites like the U.S Air Force Defense Meteorological Satellite Program – Operational Linescan System (DMSP-OLS) and its successor, the Suomi National Polar-orbiting Partnership (Suomi NPP). DMSP-OLS is a constellation of military meteorological satellites originally designed for detecting clouds at night. After its declassification in 1972, scientists realized the OLS sensor's ability to image radiance from city lights, gas flaring, fishing fleets, and other illuminated features (Croft, 1978).

Initially, socio-economic applications of NTL imagery were limited. Between the late 1970s and early 1990s, only a few studies using the data were published, namely on urban mapping (Croft, 1978; Kramer, 1994), population density (Welch, 1980) and energy usage (Sullivan, 1989). Systematic studies using NTL did not begin in earnest until 1992, when the National Oceanic and Atmospheric Administration's National Geoscience Data Center (NOAA/NGDC) created a digital archive of DMSP-OLS (hereafter referred to as OLS) data that now extends from 1992 to 2013. Prior to 1992, OLS data were not preserved or available in digital form (Elvidge et al., 1997a) and few studies used the available declassified film formats (e.g. Cahoon et al., 1992). While the satellite program is still collecting data for the military today, NOAA/NGDC are no longer digitally archiving the data because they have switched to supporting the satellite's successor, Suomi NPP VIIRS. With VIIRS data available from December 1, 2011 onward, comparison with OLS data can be made through 2013, when digital archiving of the latter product ceased.

Following the 1992 establishment of the OLS digital archive and the release of "stable lights" (non-ephemeral) composites for the United States beginning in 1997 (Elvidge et al., 1997a), researchers discovered the possibility to correlate lights with known demographic and economic variables (Elvidge et al., 1997b; Imhoff et al., 1997). From these correlations, NTL can be used to predict such variables in places where reliable statistics are otherwise lacking, like cross-border or subnational regions (Henderson et al., 2012), as the data provide a globally uniform and continuous measurement. Coincidentally, as global awareness about the effects of human activities on the environment heightened in the 1990s, a call arose for a "second environmental science" that focused on interactions between humans and the environment (Stern, 1993: 1897). From space, NTL imagery provides a useful window into these interactions while bridging areas of study that were previously the remit of either social scientists or remote sensing scientists, but not both.

A nearly twenty-year record of cross-sectional and multitemporal research has revealed strong relationships between NTL and urbanization (Henderson et al., 2003; Ma et al., 2012; Pandey et al., 2013; Zhang and Seto, 2013; Zhang and Seto, 2011), population (Elvidge et al., 1997b; Raupach et al., 2010; Sutton, 1997; Sutton et al., 2001; Zhuo et al., 2009), and national and sub-national estimates of gross domestic product (GDP) (Doll et al., 2006; Ebener et al., 2005; Sutton et al., 2007; Sutton and Costanza, 2002). NTL research is quickly advancing, too, thanks to the October 2011 launch of NASA and NOAA's Suomi NPP satellite. Its onboard Visible Infrared Imaging Radiometer Suite (VIIRS) has a Day/Night Band (DNB) specifically designed for detecting lights, meeting demands from the NTL remote sensing community for a dedicated satellite (Elvidge et al., 2007). VIIRS can detect NTL at higher spatial and radiometric resolutions than DMSP-OLS and practically eliminates three critical problems that beset the heritage satellite program: saturation, blooming, and a lack of on-board calibration. Despite these improvements, VIIRS still lacks OLS' lengthier data record, making the latter necessary for studies that extend prior to December 2011. In 2017, NASA will launch Suomi NPP's successor, the Joint Polar Satellite System-1, which will also have VIIRS onboard (Zhou et al., 2016) and therefore extend the sensor's data record.

Given these advances in NTL remote sensing technologies and applications, it is timely to review the past two decades of NTL-based examinations of socioeconomic dynamics to determine gaps in the existing and identify future directions. Accordingly, this paper examines progress in using multitemporal OLS and VIIRS imagery to detect, monitor, and predict socioeconomic dynamics at a range of spatial and temporal scales. Specific attention is given to multitemporal NTL imagery because although most research to date focuses on single-year studies (Huang et al., 2014) newer studies, including an emerging subfield in economics, explore relationships between multitemporal NTL and socioeconomic dynamics.

This paper provides an overview of multitemporal OLS and VIIRS datasets (Section 2); consideration of the main methods used in processing and correcting these data (Section 3); meta-analysis and examination of existing research and its limitations in using NTL imagery to detect and predict trends in urbanization, economic, and population dynamics (Section 4); suggestions for future research (Section 5), and concluding remarks (Section 6). Since NTL are of intrinsic interest both as a remotely sensed dataset and as a dataset that can be used to address social science questions, the two perspectives are explored and synthesized throughout the review.

2. NTL data products

2.1. DMSP-OLS

DMSP-OLS is an oscillating scan radiometer with a swath width of ~3000 km and two spectral bands: Visible Near-Infrared (VNIR), which collects NTL, and Thermal Infrared. The OLS contains two telescopes and a photo multiplier tube, which can detect radiation between 0.47 and 0.95 μm in the visible and near-infrared wavelengths (Lo, 2002). The system has a "fine" 0.56 km spatial resolution mode, but on-board averaging performed in 5 × 5 blocks sends data to NOAA/NGDC in "smooth" 2.7 km resolution. OLS has 14 daily orbits, providing global daytime and nighttime coverage every 24 h (Elvidge et al., 1999). The nighttime overpass occurs between approximately 20:30 and 21:30 (Elvidge et al., 2001). At night, OLS can detect radiances down to 1.54×10^{-9} and up to 3.17×10^{-7} $W \cdot cm^{-2} \cdot sr^{-1} \cdot \mu m^{-1}$ (Cinzano et al., 2000). Data values are reported in digital numbers (DN) on a six-bit scale that ranges from 0 (no light) to 63 (maximum reported light). OLS values are therefore relative rather than absolute measures of radiance. Since 1992, a total of nine sun-synchronous, polar-orbiting satellites named F10 through F18 have collected OLS data, with typically two contributing to the digital archive at a time. In most years, follow-

on satellite missions have collected sufficient overlapping data to allow intercalibration between different OLS sensors. For long-term studies, this type of processing is often done since OLS lacks on-board calibration and inter-satellite calibration. Section 3.1.1 describes this method.

OLS data products range from daily images to annual composites that are generated by NOAA/NGDC. Clouds, sun (especially in summer at the polar regions), and moon conditions can prevent daily orbits from detecting certain places. Cloudy days are excluded from annual composites, as are summer days when sunlight prevents imaging of NTL at latitudes farther from the equator. The costs of OLS data vary: a monthly global NTL composite, for instance, costs $7665, while annual composites are free (NOAA/NGDC, 2017a). It is possible that the high prices of daily and monthly images explain why so few studies have implemented OLS data at sub-annual timescales, though there are some key exceptions (e.g. Filho et al., 2004; Min et al., 2013). Instead, the most widely used product for multitemporal NTL studies is the global annual stable lights composites time series from 1992 to 2013 (Huang et al., 2014), included in the Version 4 DMSP-OLS NTL Series (available at http://ngdc.noaa.gov/eog/dmsp.html). Prior to release of this dataset, typically referred to as the "stable lights composites," studies relied on earlier products like the 1994–1995 stable lights product developed by Elvidge et al. (2001) or previous versions of the OLS NTL Series. Version 1 covered 1992, 1993, and 2000, while Version 2 covered 1992–2003; however, these products are no longer available for download.

The stable lights composites include all persistent lighting, assign background noise a value of 0, and reduce systematic sources of light from the sun and moon, along with more ephemeral lights like the aurora and fires (Baugh et al., 2010). Each composite is reprojected from the original orbit reference frame to constitute a 30 arc-second grid spanning 180°W to 180°E and 65°S to 75°N, covering most of the inhabited world except for the high polar regions. The composites contain light from settlements and industry, fires, gas flaring, and shipping fleets (Doll, 2008).

The Version 4 series also includes the "average visible" and "average lights times percent" annual composites. The "average visible" product averages each pixel's DN for the year without additional filtering. Although this yields fewer nonzero values for pixels, it also introduces additional noise, rendering estimates less precise (Chen and Nordhaus, 2015). The "average lights times percent" composites multiply the average DN of NTL cloud-free detections for a pixel by its percent frequency of detection within a year, meaning that the value of a DN detected for only six months is halved. These composites form the basis for the intercalibration method (Elvidge et al., 2009) described in Section 3.1.1 but are infrequently used in research. Representing one exception, Mellander et al. (2015) find that even though the "average visible" and "stable lights" products perform similarly, they are weaker than the "average lights times percent" product in estimating population and industrial activity. This finding does not appear to be widely corroborated, however, and it is worth noting that even the average visible and stable lights composites may capture industrial activity differently. For example, a visual comparison of OLS V4 average lights and stable lights products reveals a railroad in Russia's Yamal Peninsula in the former (Fig. 1a), but not the latter (Fig. 1b).

OLS data is often saturated in bright urban areas due to the collection of data at high gain settings. Depending on how urban areas are delineated, up to a third of urban pixels have been shown to be saturated at DN = 63 in the continental U.S. (Xie et al., 2014). Thus, the radiance calibrated dataset first developed by Elvidge et al. (1999) is particularly useful for studying change over time in urban areas. This product combines cloud-free OLS data obtained over 28 nights at high, medium, and low fixed gain settings in 1996 and 1997, permitting the detection of brightness variations across space in urban cores. Coverage of low-light areas, however, is weakened as a result. The units in the radiance-calibrated product are still relative due to the lack of on-board calibration and correction for interannual satellite differences (Hsu et al., 2015). Extending the work of Elvidge et al. (1999) and Ziskin et al. (2010), who create a global composite for 2006 by blending fixed-gain data with stable lights data to capture even lower levels of NTL, Hsu et al. (2015) generate a total of eight radiance-calibrated datasets for periods between 1996 and 2011 using both fixed-gain and OLS stable lights data, for which observations were collected at varying gains. There is no possibility of generating radiance-calibrated datasets for 1992–1995 since no data were collected at reduced ("low-gain") settings. These eight composites are intercalibrated to account for inter-satellite differences and sensor degradation, allowing for multitemporal comparison. Still, even this intercalibrated product only provides relative measurements and so cannot be directly compared with VIIRS. One possible way to compare and possibly even integrate OLS and VIIRS data may be to radiometrically calibrate the former using the latter (Shao et al., 2014). Additionally for the purposes of visualization, tritemporal OLS imagery can be superimposed on VIIRS data to simultaneously visualize decadal change in lights and more precise brightness values (Small and Sousa, 2016).

2.2. Suomi NPP VIIRS DNB

Suomi NPP was launched on October 28, 2011 and has five Earth-observing sensors, including VIIRS. This multispectral sensor has 22 bands, with the DNB capturing NTL data – arguably VIIRS' most innovative feature (Hillger et al., 2013). VIIRS' spatial resolution of 742 m, preserved across a ~3040 km swath width, is 45 times higher than OLS at nadir and 88 times higher at scan edge. Its radiometric resolution is 256 times finer and its sensitivity to radiance 10 times higher (Miller et al., 2013). VIIRS' ability to resolve lower light levels at smaller intervals, with a measured spectral response of 505–890 nm full width at half maximum (fwhm) (Miller et al., 2012), represents a significant advance over OLS. To put this in perspective, VIIRS' high radiometric sensitivity enables it to differentiate between 1 km^2 that is lit by a single street lamp and one that is not (Seaman and Miller, 2015). While OLS data have been shown to be strongly correlated with ground-based measurements of NTL (Kyba et al., 2013), VIIRS is expected to produce even stronger correlations (Katz and Levin, 2016).

However, VIIRS still falls short of specific calls for a NTL satellite with medium spatial resolution (~50 m) and multispectral bands (Elvidge et al., 2007), for the DNB merely collects information across a single wide spectral band. Furthermore, VIIRS is not superior to OLS in all aspects. As some cities begin to switch from high-pressure sodium to more energy-efficient white light-emitting diode (LED) lighting, VIIRS will erroneously detect a reduction in light pollution because of its insensitivity to wavelengths below 500 nm, the bluish part of the spectrum where LEDs emit a substantial amount of light (Falchi et al., 2016). OLS, whose slightly wider wavelength ranges from 0.4 to 1.1 μm, may have a better chance at detecting LED lighting.

VIIRS data has 12- or 14-bit quantization depending on noise levels and are reported in radiance in units of nanoWatts/($cm^2 \cdot sr$). While VIIRS' specified dynamic range lies between 3×10^{-9} to 0.02 $W \cdot cm^{-2} \cdot sr^{-1}$, actual performance puts the noise floor at 5×10^{-11} $W \cdot cm^{-2} \cdot sr^{-1}$, allowing detection of extremely faint point sources of light (Cao and Bai, 2014). Its three gain stages allow detection of a greater dynamic range of radiance during the day, twilight, and night (Miller et al., 2012). The overpass time occurs approximately after 1:30 am local time (Elvidge et al., 2013a), when there is generally less illuminated activity occurring on the ground than during the 20:30–21:30 overpass time of OLS. This difference should be kept in mind when comparing data from the two satellites (Table 1).

Gathered by a satellite jointly operated by NASA/NOAA as opposed to the U.S. Department of Defense, VIIRS data are freely available to the public. This opens the door to a range of studies using multitemporal NTL imagery, including at sub-annual time scales costly to study with DMSP-OLS data. Raw VIIRS data granules, which include the sensor data records and geolocation information, are available from a number of websites such as NOAA's Comprehensive Large Array-Data

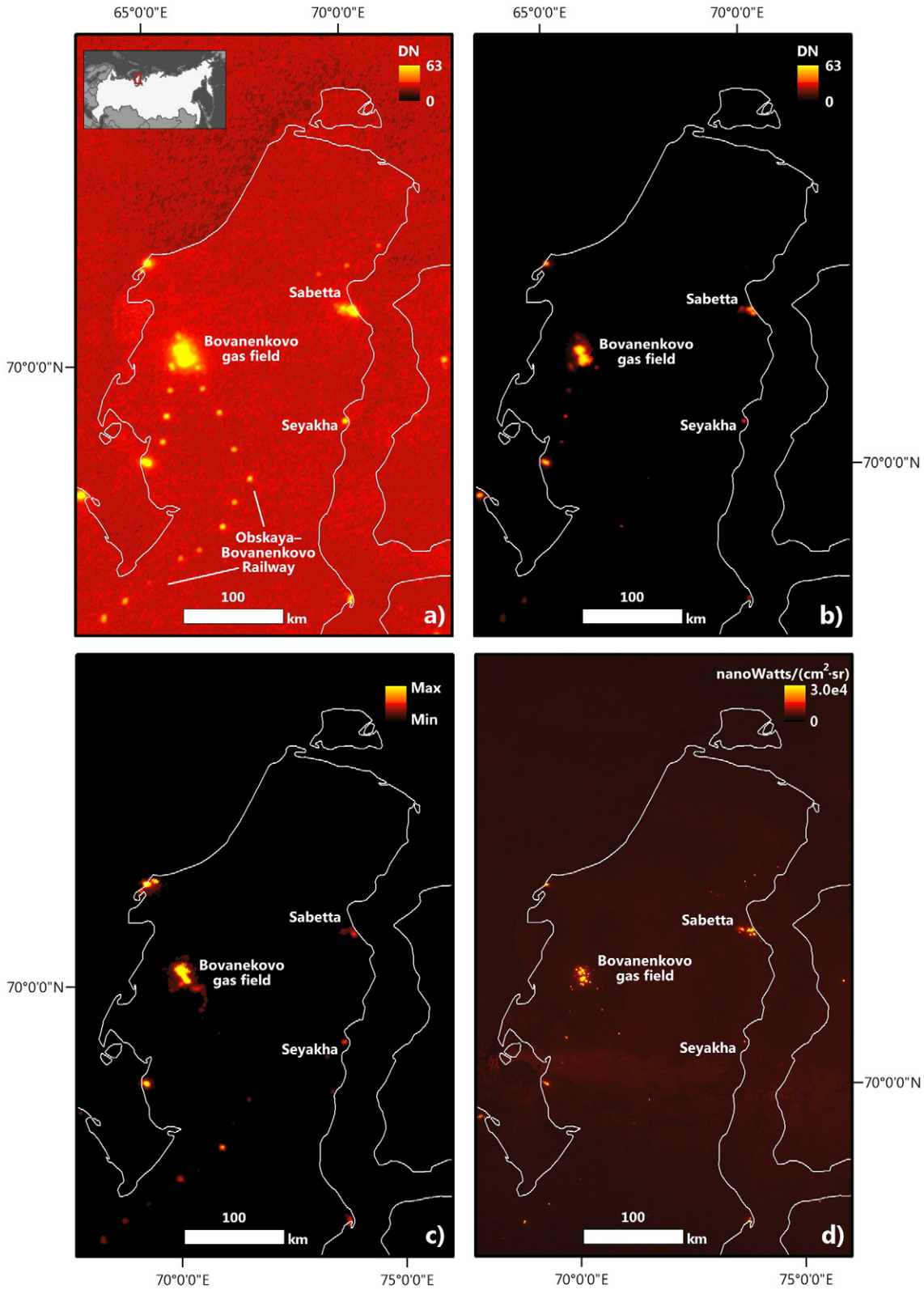

Fig. 1. a) OLS V4 Average Lights Composite for 2013 of the Yamal Peninsula in Russia, an area undergoing natural gas development. b) OLS V4 Stable Lights Composite for 2013. The railway is less visible. c) OLS Radiance Calibrated Lights composite for 2010/2011, where railway stations are visible. d) Version 1 Nighttime VIIRS DNB Composite for November 2014 reveals improved spatial resolution and more accurate delineation of lit areas, which represent gas flares, settlements, and industrial sites. Map projection: Asia North Albers Equal Area Conic.

Stewardship System (CLASS) (http://www.nsof.class.noaa.gov) and the University of Wisconsin's NASA Atmosphere SIPS server (http://sips.ssec.wisc.edu/). NOAA's Earth Observation Group distributes processed global- and regional-level data, including the VIIRS NTL 2012 product and the monthly Version 1 (V1) Nighttime VIIRS DNB Composites. Like the OLS composites, both VIIRS products stretch from 65°S to 75°N, though they are divided into a total of six 15 arc-second geographic grids rather than provided as a single GeoTIFF with global

Table 1
DMSP-OLS VNIR Band compared with Suomi NPP VIIRS Day/Night Band.

Satellite (and NTL imaging band)	DMSP-OLS (VNIR Band)	Suomi NPP (VIIRS DNB)
Operator	U.S. Department of Defense	NASA/NOAA
Available years of digital data	1992-present, but new annual composites are not being made available after 2013	December 2011-present
Wavelength range	0.4–1.1 μm	505–890 μm
Spatial resolution	2.7 km	742 m
Temporal resolution	12 h	12 h
Geographic extent	75N/65S/180E/180W	75N/65S/180E/180W
Specified day/night overpass time	8:30–9:30 and 20:30–21:30	13:30 and 1:30
Radiometric resolution	6-bit	12- or 14-bit
Units measured	Relative (0–63 scale)	Radiance (nanoWatts/($cm^2 \cdot sr$)
Light ceiling	3.17×10^{-7} W·cm^{-2}·sr^{-1}·μm^{-1}	0.02 W·cm^{-2}·sr^{-1}·μm^{-1}
Light floor	1.54×10^{-9} W·cm^{-2}·sr^{-1}·μm^{-1}	3×10–9 W·cm^{-2}·sr^{-1}·μm^{-1} (specified; lower values have been detected)
On-board calibration	No	Yes

coverage. The VIIRS NTL 2012 product was the first cloud-free composite made from data from the new sensor. Released in early 2013, it contains observations made on moonless nights between April 18–26 and October 11–23, 2012. No comparable products for subsequent years yet exist that would allow for interannual comparisons.

The VIIRS V1 composites constitute monthly global average radiance composite images in which cloud cover, lightning, and lunar illumination are eliminated (Mills et al., 2013). Two configurations of the V1 composites are available: a first, called "vcmcfg," which excludes data affected by stray light that enters through the sensor's scan cavity, and a second, called "vcmslcfg," which includes such values after they are corrected for stray light following the method described in Mills et al. (2013). This second configuration is of poorer quality but contains more data coverage near the poles. For both configurations, the number of cloud-free observations used to create each pixel within a monthly composite is provided as a separate image. The V1 VIIRS composites are available for every month from April 2012 onward. Unlike the OLS V4 stable lights composites, aurora, fires, and other ephemeral lights are still included in the V1 VIIRS composites since a robust method of removing them is under development (NOAA/NGDC, 2017b). Generally compared to the heritage satellite, however, VIIRS can more readily distinguish between electric lighting and combustion with appropriate algorithm development (Elvidge et al., 2013a) and between cloud, snow cover, and snow-free land (Lee et al., 2006).

Fig. 1 compares three types of DMSP-OLS composites and a monthly VIIRS composite of Russia's Yamal Peninsula, which lies above the Arctic Circle. Settlements, industrial areas, and gas flares emanating from the peninsula's natural gas industry are more clearly delineated in the VIIRS image, illustrating its improved spatial resolution and reduced blooming (Hillger et al., 2013; Miller et al., 2013; Miller et al., 2012). Saturation is also much reduced, too. VIIRS captures large and slight spatial fluctuations in anthropogenic lighting, especially in the rural-urban transition zone and in urban cores where OLS data tends to be saturated (Ma et al., 2014c). As a comparison of images of New York City reveals, VIIRS (Fig. 2b) better resolves urban structure and connectivity by detecting both small, dim lights and bright lights without saturation or attenuation (Small et al., 2013). In the OLS image (Fig. 2a), the city appears saturated and blooms over the surrounding rivers. In the VIIRS image, it is possible to distinguish brighter and dimmer spots in Manhattan, like downtown and Central Park, respectively. From the snowy and watery circumpolar north to densely populated coastal cities, VIIRS' improvements can assist with examining socioeconomic parameters and dynamics.

3. Data processing and interpretation for multitemporal analysis

Drawing inferences from NTL data, particularly OLS, poses challenges due to three key issues originating from the satellite: a lack of on-board calibration, blooming, and saturation (Imhoff et al., 1997; Small et al., 2011; Small et al., 2005). A major issue that originates from the ground is gas flaring (Elvidge et al., 2009). In order to process NTL imagery for cross-sectional or multitemporal analysis, a number of corrections are necessary, which this section reviews. Two of the most common ways to interpret changes in NTL are also explored: changes in intensity versus lit extent.

3.1. Data processing

3.1.1. Intercalibration and fixed effects

From one year to the next, the performance of an OLS satellite changes due to sensor degradation (Zhang and Seto, 2011). A different OLS satellite may also capture data altogether. The two main methods of reducing measurement errors due to interannual satellite differences are intercalibration (Elvidge et al., 2009) and year fixed effects (Henderson et al., 2012). Remote sensing scientists tend to apply the former method while economists include the latter in their models.

Intercalibration is possible because there is generally at least one year of overlap between any single OLS satellite and its replacement. Still, the method cannot correct for the fact that although the overpass times are meant to occur at the same time of day and night for each satellite, actual overpass times may vary by up to two hours between satellites (Elvidge et al., 2009). This can result in different NTL measurements due to changing ground conditions. Using the "average lights times percent" composites, Elvidge et al. (2009) developed the most widely used intercalibration method. Operating under the assumption that the relationship between NTL in a given year and in 1999 is quadratic, an ordinary least-squares regression model is used to intercalibrate the data as:

$$\mathrm{DNadjusted} = C_0 + C_1 \times \mathrm{DN} + C_2 \times \mathrm{DN}^2$$

with C_0, C_1 and C_2 the empirically estimated coefficients (provided in Elvidge et al. (2009)), DN the original pixel value, and DN adjusted the resulting adjusted pixel value. All composites are intercalibrated to match the values in the F12999 composite, as it has the highest average DN values. To estimate their intercalibration coefficients, Elvidge et al. (2009) use Sicily as their reference area since it radiates light over the full spectrum of values and is assumed to have experienced minimal lighting change over the years. After intercalibration, Sicily retains similar DN adjusted values from one year to the next. Other researchers have modified this method by changing the reference area to a location within their study area where lighting is assumed to be stable across time (Liu et al., 2015a; Pandey et al., 2013). Chen and Nordhaus (2011) draw attention to the fact that many researchers adopt the intercalibration method not for comparing the "average lights times percent" composites upon which it was originally based, but rather the stable

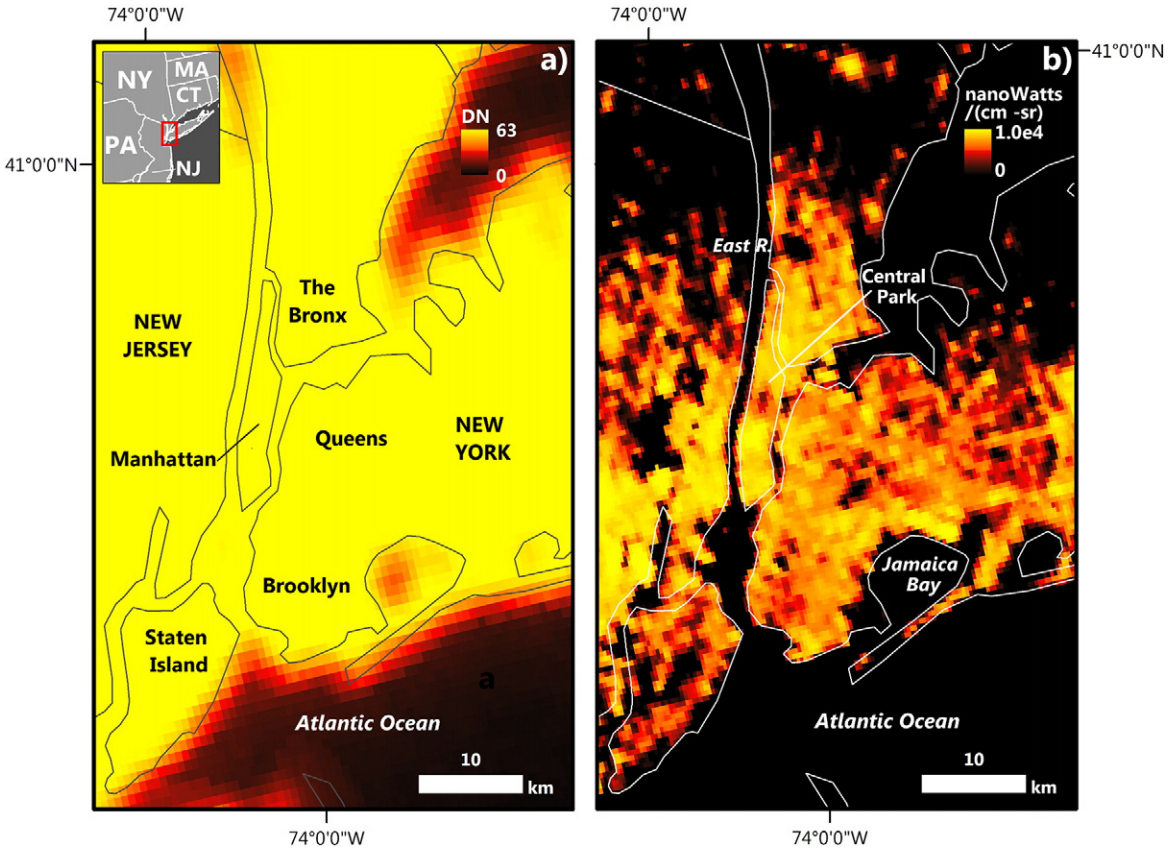

Fig. 2. a) OLS V4 Stable Lights Composite for 2013 over New York City and environs. Saturation and blooming over water are readily apparent. b) Version 1 Nighttime VIIRS DNB Composite for January 2014. Notice the reduced saturation and blooming and ability to distinguish between darker (Central Park, East River) and brighter areas within an area that appears saturated in the OLS imagery. As the OLS V4 Average Lights Composite and DMSP-OLS Radiance Calibrated Lights composite look nearly identical to the Stable Lights Composite, they are not included in this figure. Map projection: North American Lambert Equal Area.

lights composites. However, they test the intercalibration method in Elvidge et al. (2009) on the stable lights composites and conclude that the results are satisfactory.

As an alternative method of calibrating DMSP-OLS composites, Bennie et al. (2014, 2015) use a robust regression technique called quantile regression on the median. Compared to the OLS-based method of Elvidge et al. (2009), their technique is less influenced by outliers and assumes that at least 50% of pixels within the reference area maintain constant brightness rather than all of them. Quantile regression on the median may therefore be more appropriate for places experiencing limited directional change in lighting over time (Bennie et al., 2014). For their intercalibration method, the F101994 composite serves as the base year since it has the highest proportion of pixels with the minimum and maximum values (0 and 63).

While most multitemporal studies examine interannual change, comparison of monthly composites benefits from controlling for seasonal factors. To diminish the effects of predictable, seasonal factors like vegetation variation and lunar illumination, Letu et al. (2015) create a time-series of 10-day data for 1999 by compositing the maximum digital numbers. To remove seasonal periodic noise, they extend the noise reduction filter developed by Hara et al. (2010). Their method also helps counter underestimation of DNs due to persistence of thin clouds.

Many economists using NTL data forego intercalibration and instead control for year fixed effects (Chen and Nordhaus, 2011, 2015; Henderson et al., 2012). Henderson et al. (2012) seek to use lights in a predictive manner by obtaining a regression of income growth versus NTL growth. They estimate a log-linear model between the "sum of lights" (a common measure in the literature which adds all of the digital values of the pixels in a given area, hereafter referred to as "SOL") for each country and its GDP. The model includes an error structure that includes year fixed effects, which is written as:

$$\tilde{e}_{jt} = c_j + d_t + e_{jt}$$

for which $\tilde{e}$ is the error for country j in year t, c_j is country fixed effects (controlling for factors like differences in lighting patterns and investment in outdoor lighting, which are unrelated to intercalibration), d_t is year fixed effects (controlling for interannual satellite differences and changes in global external conditions, like technology and economic activity), and e_{jt} is the remaining error. Unlike intercalibration, which can be applied to NTL data by itself, controlling for fixed effects requires the availability of an alternative quantity of interest, like GDP. This method would therefore not be useful for examining interannual NTL trends in a place for which no ancillary data are available. For instance, to simply make a change detection map of NTL in a remote stretch of desert from 1992 to 2012, intercalibration would be the more applicable method to correct for satellite differences.

3.1.2. Saturation

Saturation, sometimes called top-coding (Henderson et al., 2012), is one of the primary limitations with OLS data as it has only 8-bit quantization and low dynamic range. Therefore, the sensor cannot measure brightness levels beyond a value of 63 DN. This is especially problematic for studies of brightly lit urban cores, as saturation prohibits the detection of variation in lighting levels beyond DN = 63 (Small et al., 2005).

In the United States, East Asia, and Western Europe, many metropolitan cores have reached saturation, making further brightening undetectable with OLS imagery. In mainland China alone, Ma et al. (2014b)

identify 135 saturated cities. Some studies examine multitemporal NTL imagery without correcting for saturation effects (Chand et al., 2009; Zhang and Seto, 2011). This is acceptable when most light sources fall under the saturated value, as in India (Chand et al., 2009) or Africa, where between 2007 and 2008, a mere 0.00017% of lit pixels were saturated (Michalopoulos and Papaioannou, 2013). However, studies foregoing saturation correction that use NTL as a continuous measure without ensuring that there are no saturated pixels should be assessed critically.

Saturation corrections are essentially irrelevant for studies that simply threshold NTL, but they are necessary for those that use NTL as a continuous measure. When applied, saturation corrections can improve the accuracy of results in studies of long-term socioeconomic trends using OLS data (Letu et al., 2012). Several methods have been suggested. Raupach et al. (2010) propose a probabilistic saturation correction, estimating that NTL intensity (DNs) should be multiplied at the regional scale by an average of 1.15 (ranging from 1.003 for "least developed countries" to 1.570 for Japan, a densely urbanized country with significant saturation) and at the cell scale by an average of 1.23. Letu et al. (2010) find that at a 1-km^2 resolution within nine electric power supply areas in Japan, the median daily DN is linearly correlated with built area. Consequently, they estimate the actual values of saturated areas using a cubic regression equation. Applying this correction for saturated light improves the fit between stable lights and electric power consumption in Japan and 12 other countries in Asia. Letu et al. (2012) enhance this method by finding a strong linear correlation ($R^2 = 0.93$) between the SOL of unsaturated areas in both stable light and radiance-calibrated images. They derive a regression function that more accurately estimates the true values of saturated pixels. This new method modestly improves the correlation between regional SOL in the stable lights image and annual electric power consumption from $R^2 = 0.81$ derived using Letu et al.'s (2010) method to $R^2 = 0.91$. Lastly, after evaluating two regional-level and two pixel-level saturation correction methods, Ma et al. (2014b) conclude that the correction should be chosen depending on the study area. Regional-level methods are appropriate for correcting data in areas with many saturated pixels, while pixel-level correction methods are more appropriate for areas with fewer saturated pixels.

3.1.3. Blooming

Blooming (also called spatial blurring or overglow) occurs when the averaging of adjacent input cells to produce output cells causes lit pixels to extend beyond a source's true illuminated area. This issue is especially acute in OLS imagery (Xie et al., 2014) and is more pervasive over water and snow areas, as these reflect nearby lights more than dark ground. Two-fifths of the world's major cities with populations of 1–10 million are located near coastlines (Tibbetts, 2002). Since cities form a popular topic for NTL-based studies, blooming should be of particular concern when examining coastal metropolises, though blooming can occur over land, too. Failing to correct for blooming when using NTL as a proxy can result in overestimation of features such as urban extent, since changes in brightness tend to be bigger in area than associated land cover changes (Small and Elvidge, 2013). Typically, blooming is proportional to the SOL emitted by a light source, such as an urban area. In Australia, Townsend and Bruce (2010) find a strong correlation between a city's SOL and the spread of its lights past the coastline for nine coastal cities ($R^2 = 0.89$).

There is little consensus on how to correct for blooming. Thresholding, whether based on a detection frequency or a fixed or scaled DN value, can reduce the effect of blooming and is the most widely investigated method. Yet there is little agreement on how exactly to apply it (Zhou et al., 2014). Based on an examination of urban areas in the U.S., Imhoff et al. (1997) conclude that a frequency detection threshold selecting pixels lit in 89% of the orbital passes contained within the 1994/1995 DMSP-OLS stable lights composite results in more accurate urban boundaries when compared with 1990 U.S. Census data on urban areas and eliminates blooming. However, this threshold makes many small settlements disappear. Showing how thresholds can vary from city to city, Henderson et al. (2003) determine that the stable lights images of Beijing, Lhasa, and San Francisco are most accurately thresholded at frequency detection levels of 97%, 88%, and 92%, respectively. Also differing from Imhoff et al. (1997)'s claim of the effectiveness of a uniform threshold of 89%, Small et al. (2005) examine 17 cities worldwide in the 1992/1993, 1994/1995, and 2000 stable lights datasets and determine that no single threshold produces spatial extents consistent with Landsat-derived built extent. They instead suggest employing a scale-dependent blooming correction procedure that accounts for the size of the lit area. After imposing a linear relationship between lit area and blooming extent for 10 illuminated islands, they suggest that a scale-dependent correction for blooming may be effective. However, no further research has been conducted on this method's effectiveness and it is unclear whether it would work over non-coastal areas. Finally, the Overglow Removal Model (ORM) developed by Townsend and Bruce (2010) considers the effects of annual atmospheric conditions, topography and elevation, and differences in regional lighting technologies on the extent and influence of blooming. Yet as this information is not always available, especially for locations in developing areas where applications of NTL imagery may provide the most insight, the ORM's applicability may be limited.

Due to the challenges posed by blooming and interpreting very low DN values, the choice of threshold may significantly affect the outcome of many NTL studies whether they measure the intensity or extent of lights. Yet similar to how there is no consensus on a globally uniform standard for a detection frequency threshold to delimit urban areas, there is also no consensus on a globally uniform standard DN threshold. Illustrating the range of DN-based thresholds used in NTL studies, Yi et al. (2014), use DN > 10 to delimit urban areas in China, while Amaral et al. (2006) use DN > 30 to delimit urban areas in the Brazilian Amazon. Based on validation against high-resolution land-cover data, Zhou et al. (2014) find that the optimal DN threshold for delineating large urban clusters like Boston and Beijing is 60, while it is 20 in smaller cities. Optimal thresholds for extracting lit urban area can even vary within one country and over time (Gao et al., 2015). Small et al. (2011) suggest that spatial extent and intensity of development, as proxied by NTL, are continuous rather than discrete in nature and exhibit distinct spatial phase transitions. As the threshold increases from 3 to 60, networks of lit area fragment and shrink due to the exclusion of dimmer lights connecting these regions. The decrease in delineated lit area at a threshold of DN = 8 suggests both a strong sensitivity to delineation of lit area at low DN thresholds (DN < 8) and a sharp decrease in the global frequency distribution of lights around DN = 8. Given the range of potential thresholds that can be used, research that employs thresholding as a method of analysis should also report the sensitivity of results to changes in the value of the threshold.

VIIRS data hardly exhibit any blooming in comparison to OLS and hence require few, if any, corrections. In one of the few studies so far that examines blooming in VIIRS versus OLS, Xie et al. (2014) first normalize an image from each dataset (the 2012 OLS V4 composite and a two-month VIIRS composite from 2012) using a linear stretch to make them comparable. They find that extracting the same sized urban area from these two images requires 4000 continuous lights in the OLS image and 23,000 in the VIIRS image. This is because VIIRS data fragment large urban areas and capture additional small urban areas. Saturation or blooming may affect resolution of these features in OLS. Overall, thanks to the reduction in blooming, VIIRS imagery now depicts brightly lit coastal conurbations like the Northeastern U.S. as a fine web of interconnected cities rather than a blob of light in OLS imagery (Ou et al., 2015).

At the same time, VIIRS' lower limit allows detection of nocturnal airglow, the background luminosity emitted by the Earth's ionosphere (Elvidge et al., 2013a). OLS has not demonstrated an ability to detect this airglow due to its lower sensitivity (Miller et al., 2012). Since airglow varies around the Earth, Kyba et al. (2015) caution that these

Table 2
Representative examples of studies using multitemporal OLS or VIIRS imagery.

Publication year	NTL dataset	Time range	Time step	Variable of interest	Universe of analysis	Scale/Unit of analysis	Measure of NTL	Data transformation	Method of controlling for satellite differences across years	Main mathematical or statistical approach/model	Ancillary data	Author(s)	Title	Journal
2004	Daily DMSP-OLS VNIR and TIR images	July 23–July 24, 1999; 24–26 January 2001	Daily	Urban damaged area	Taiwan; Western India	Pixel	DN	None (daily)	N/A	DN differences	None	Kohiyama, M., Hayashi, H., Maki, N., Higashida, M., Kroehl, H.W., Elvidge, C.D., Hobson, V.R.	Early damaged area estimation system using DMSP-OLS night-time imagery	International Journal of Remote Sensing
2007	1992/1993 and 2000 DMSP-OLS city lights composites	1992/1993–2000	17/18 years	GDP	India, China, Turkey, and the U.S.	Subnational regions	SOL and lit extent	Log	None	Linear regression	Landscan population and sub-national GDP figures	Sutton, P., Elvidge, C., Ghosh, T.	Estimation of gross domestic product at sub-national scales using nighttime satellite imagery	International Journal of Ecological Economics and Statistics
2011	DMSP-OLS V4 stable lights composites (along with raw and radiance calibrated versions for sensitivity checks)	1992–2008	Annual	GDP	Global	Country-level and 1 × 1 grid-cell level	SOL	Log	Fixed effects	Cross-sectional and panel regression	World Bank GDP PPP data; G-Econ 3.4 cell data	Chen, X., Nordhaus, W.D	Using luminosity data as a proxy for economic statistics	Proceedings of the National Academy of Sciences
2011	DMSP-OLS V4 stable lights composites	1992–2008	Two years	Urban area	Global and China, India, Japan and the U.S.	1-km^2	SOL	Normalization	None	Linear regression	1992–2001 Land Cover Change Retrofit Product	Zhang, Q., Seto, K.C.	Mapping urbanization dynamics at regional and global scales using multi-temporal DMSP/OLS nighttime light data	Remote Sensing of Environment
2012	DMSP-OLS V4 stable lights composites	1992–2008	Annual and 1992/1993 vs. 2005/2006 and 2007/2008 (13–16 years)	GDP	Global	Subnational, national, and supranational levels	Weighted average of lights across pixels in a country (each pixel's weight = share of its country's land area)	Log	Fixed effects	Panel regression	Economic and population measures from World Development Indicators	Henderson, J.V., Storeygard, A., Weil, D.N.	Measuring economic growth from outer space	American Economic Review
2012	DMSP-OLS V4 stable lights composites	1994–2009	Annual	Urbanization	China	Cities	Weighted light area	None	Intercalibration	Linear, power-law, and exponential regression	Urban population, GDP, urban built-up area, and electric power consumption from National Bureau of Statistics of China	Ma, T., Zhou, C., Pei, T., Haynie, S., Fan, J.	Quantitative estimation of urbanization dynamics using time series of DMSP/OLS nighttime light data: a comparative case study from China's cities	Remote Sensing of Environment
2013	2009 FMSP-OLS V4 F16 annual stable and	2009 and 2011	Daily, monthly, and yearly	Rural electrification	Senegal and Mali	Villages	DN	None	Fixed effects	Panel regression	Survey and administrative data on	Min, B., Gaba, K.M., Sarr, O.F., Agalassou, A.	Detection of rural electrification in Africa using	International Journal of Remote

(continued on next page)

Table 2 (*continued*)

Publication year	NTL dataset	Time range	Time step	Variable of interest	Universe of analysis	Scale/Unit of analysis	Measure of NTL	Data transformation	Method of controlling for satellite differences across years	Main mathematical or statistical approach/model	Ancillary data	Author(s)	Title	Journal
	average lights composites, April and May 2011 DMSP F18 monthly average lights composites, April 18–June 15, 2011 DMSP F18 nightly visible lights										electricity use and electrification		DMSP-OLS night lights imagery	Sensing
2013	DMSP-OLS V4 stable lights composites	1992–2009	Annual	Urbanization	Colombia, Ecuador, Peru, Bolivia	Municipal, national and regional levels	Minimum/maximum DN value in municipality	None	None	Linear regression	Census population data; Google Earth's Quick Bird and IKONOS images	Álvarez-Berríos, N.L., Parés-Ramos, I.K., Aide, T.M.	Contrasting patterns of urban expansion in Colombia, Ecuador, Peru, and Bolivia Between 1992 and 2009	Ambio
2013	DMSP-OLS V4 stable lights composites	1999–2009	Annual	Structure and form of cities	Global	0.05° cells and 11 × 11 and 21 × 21 grids centered on 100 large cities	Average DN in each cell	None	Intercalibration	*k*-means cluster analysis	MODIS 500m map of Global Urban Extent and NASA SeaWinds microwave scatterometer mean summer backscatter power ratio	Frolking, S., Milliman, T., Seto, K.C.	A global fingerprint of macro-scale changes in urban structure from 1999 to 2009	Environmental Research Letters
2014	DMSP-OLS V4 stable lights composites	1992–2009	Annual	Regional favoritism	Global	Subnational regions	Average NTL intensity plus 0.01 per region	Log	Country-year fixed effects	Panel regression	CIESIN boundaries, Archigos database of political leaders, additional data on "political institutions, schooling, GDP, linguistic diversity, the strength of family ties, foreign aid inflows, and oil rents"	Hodler, R., Raschky, P.	Regional favoritism	The Quarterly Journal of Economics
2014	Suomi VIIRS DNB daily imagery	2012–2014	Daily	Total lighting electricity usage during holidays	North America and the Middle East	Cities	Radiance	No	N/A	Multiple regression	Daily electric load profiles	Román, M.O., Stokes, E.C.	Holidays in lights: tracking cultural patterns in demand for energy services	Earth's Future

2015	DMSP-OLS V4 stable lights composites	1992–2012	Annual	Urbanization	China	National, provincial, and county levels	Compounded Night Lights Index (average NTL brightness of all pixels in region × proportion of lit urban areas to total area of region)	No	Intercalibration, intra-annual composition and inter-annual series correction	Linear regression	Socioeconomic census data from China Population and Employment Statistics Yearbook, China Statistical Yearbook, and China City Statistical Yearbook	Gao, B., Huang, Q., He, C., Ma, Q.	Dynamics of urbanization levels in China from 1992 to 2012: perspective from DMSP/OLS nighttime light data	Remote Sensing
2015	DMSP-OLS V4 composites (type unspecified)	1992–2013	Annual	Population	Global	Pixel-level, areas around streams and rivers, continents, and countries	Absolute and relative SOL	No	Intercalibration	Linear regression	HydroSHEDS river network dataset	Ceola S, Laio F and Montanari A	Human-impacted waters: new perspectives from global high-resolution monitoring	Water Resources Research
2015	DMSP-OLS annual composites (version and type unspecified)	1992–2009	Annual	GDP (especially of agriculture and forestry)	Global	30 arc-sec grid cell, country and district (agricultural and non-agricultural) levels	Light/area	Log	Fixed effects	Panel regression	MODIS yearly land cover product MDC12Q1 and World Development Indicators	Keola, S., Andersson, M., Hall, O.	Monitoring economic development from space: using nighttime light and land cover data to measure economic growth	World Development
2015	DMSP-OLS V4 composites (type unspecified)	1992–2012	Annual	Population	Europe	Countries	Lit area	No	Intercalibration	Correlation	World Bank GDP and population data	Archila Bustos, M.F., Hall, O., Andersson, M.	Nighttime lights and population changes in Europe 1992–2012	Ambio
2015	Suomi NPP VIIRS monthly composites	May–December 2014	7 months	Electricity shortages due to insurgency	Iraq	Urban areas	SOL	No	N/A - determined not necessary for monthly composites	Descriptive statistics	MODIS 500m map of Global Urban Extent and media sources	Xi, L., Zhang, R., Huang, C., Li, D.	Detecting 2014 Northern Iraq Insurgency using night-time light imagery	International Journal of Remote Sensing
2016	DMSP-OLS annual composites (version and type unspecified)	1992–2011	Annual	Size of informal economic activity	Cambodia	Grid-level within district-level administrative boundaries	Adjusted light intensity and adjusted light share (proportion of lit area relative to total land area)	Log	Light-scaling factors	Panel regression	Business registration data from the Economic Census of Cambodia	Tanaka, K., Keola, S.	Shedding light on the shadow economy: a nighttime light approach	Journal of Development Studies

variations should be taken into account when creating a VIIRS DNB stable lights product. Failure to do so could cause certain regions with persistently enhanced airglow to be observed as brighter than they actually are, reducing reliable prediction of socioeconomic variables from lights at a globe scale.

3.1.4. Gas flares

Gas flaring is an industrial practice that results from the combustion of gas at oil production sites that cannot be economically shipped out to market. Gas flares over the Yamal Peninsula in Russia, one of the world's biggest gas flarers, are visible in Fig. 1. While the OLS V4 stable lights composites contain gas flares, these should generally be removed during pre-processing so as not to affect estimates of socioeconomic variables unless research is specifically examining the phenomenon (e.g. Elvidge et al., 2009). Gas flaring can also be used to approximate carbon emissions (Doll et al., 2000; Ou et al., 2015), but in many other studies such as of population estimates, their inclusion can introduce inaccuracies. For instance, a study using change in NTL over time in Nigeria, another major gas flarer, to predict economic or population growth would be complicated by the activity's strong persistence. Original efforts to use NTL imagery to identify and reduce gas flaring began in 2003 when the World Bank established the Global Gas Flaring Reduction Partnership. Since oil and gas companies' statistics on flaring were unreliable, the World Bank and NOAA partnered to use OLS imagery from 1995 to 2006 to create the first globally consistent satellite survey of gas flaring (World Bank, 2011: 8). The effort also eventually led to the release of the NOAA/NGDC Global Gas Flaring Shapefiles, which encompass most gas flares for the year 2008 (http://ngdc.noaa.gov/eog/interest/gas_flares_countries_shapefiles.html) and can be used to mask out gas flares in stable lights composites. However, some areas that represent actual anthropogenic lighting are included in these polygons (Cauwels et al., 2014); Henderson et al. (2012) find that these polygons include 0.3% of world population. It is unclear whether the NOAA/NGDC gas flare shapefiles provided for use with OLS should be used with VIIRS given the latter's higher spatial resolution and the years that have passed since the shapefiles' creation. Gas flares in Russia's Yamal Peninsula illustrated in Fig. 1, for instance, appear as several small, distinct light sources in the VIIRS image compared to appearing as one large, nucleated light source in the three OLS images. Recent efforts to use VIIRS to identify gas flaring (Elvidge et al., 2015; Elvidge et al., 2013b) could allow updating of these shapefiles. In sum, while gas flaring still requires correcting in studies using VIIRS data to estimate population or other variables unrelated to the activity, the need for intercalibration and corrections for blooming and saturation are almost entirely reduced.

3.2. Data interpretation

3.2.1. Changes in NTL intensity and extent

Changes in NTL may be the result of actual increases or decreases in artificial lighting that are tied to variables like population or GDP, making them a useful proxy for socioeconomic studies. At the pixel level, NTL is represented by a digital number (DN) in OLS and actual radiance in VIIRS. At larger scales, total NTL intensity is typically measured as the SOL; some derivatives include the average (rather than total) SOL within an area, per capita SOL, and weighted lit area, defined as the "sum of the areas of lit pixels multiplied by the normalized DN value" (Ma et al., 2012: 101). NTL extent is often simply measured as the total area above or below a certain threshold, but as discussed in Section 3.1.3, the choice of threshold can significantly affect results.

While NTL intensity and extent may in certain circumstances grow in parallel, the factors affecting one do not always affect the other. Lights can grow in intensity without increasing in extent and vice versa. The choice of one measure over another can therefore also affect results. For instance, delineating a change in urban area based on change in the amount of lit area would likely detect cities that had expanded outwards. In contrast, measuring a change in urban area based on pixels that have increased in brightness would be more likely to capture cities that had expanded upwards or become denser. Furthermore, it should be kept in mind that changes in NTL may also be caused by alterations in the color, type, or spectra of lighting used. Bennie et al. (2014) identify locations in Europe where deliberate energy and cost savings strategies rather than economic decline led to reductions in light emissions.

A handful of studies use lit area in some form (Doll and Pachauri, 2010; Elvidge et al., 1997b, 1997c; Sutton et al., 2007). This measure can be useful when only the absence or presence of NTL is of interest, for instance to study access to electricity (Doll and Pachauri, 2010). Yet a majority of studies use SOL to measure NTL change. In a study of 35 cities in China using the 1996/1997 radiance calibrated DMSP-OLS image, Lo (2002) finds that SOL is more highly correlated than lit area with nonagricultural population ($R^2 = 0.91$ vs. $R^2 = 0.78$), GDP ($R^2 = 0.91$ vs. $R^2 = 0.70$), built-up area ($R^2 = 0.91$ vs. $R^2 = 0.84$), and electricity consumption ($R^2 = 0.86$ vs. $R^2 = 0.77$). While SOL may be the preferred measure for examining socioeconomic variables, in some circumstances, especially in saturated areas, measures derived from lit area are shown to be preferable. Sutton et al. (2007) determine that a more complex spatial analytic approach combining lit area with population data rather than summing NTL more accurately estimates sub-national GDP within all four of their country case studies (China: $R^2 = 0.96$ vs.0.94; India: $R^2 = 0.84$ vs. 0.70; Turkey: $R^2 = 0.95$ vs. 0.58; U.S.: $R^2 = 0.72$ vs. 0.70).

3.2.2. Spatial scale

Making inferences about socioeconomic parameters from NTL imagery requires attention to spatial scale. One challenge is the Modifiable Area Unit Problem, which occurs when different results are observed from the same data at varying spatial resolutions (the scale effect) or when the scale remains the same but variations in zoning boundaries lead to different results (the zoning effect) (Doll et al., 2006). Scale effects can lead researchers to commit an ecological fallacy by making erroneous inferences from coarse-resolution data about finer-scale processes. For example, just because California's mean NTL is brighter than Nevada's does not necessarily imply that Los Angeles and San Francisco are brighter on average than Las Vegas.

While several studies examine NTL across scales (Doll et al., 2006; Forbes, 2013; Gao et al., 2015; Ma et al., 2014a; Small et al., 2005), variations in relationships across scales are not always adequately explained. From 1992 to 2012, Gao et al. (2015) find R^2 values between a composite urbanization index and compound NTL index (the average DN of all pixels in a given spatial unit in China multiplied by the proportion of the unit's lit urban area out of its total area) of 0.96 at the national scale, 0.71 at the provincial scale, and 0.69 at the county scale. They suggest that the extraction of urban lit area by thresholding at the coarser scale of the region (in between the national and provincial scales) may be responsible for the weaker correlations found at finer scales. NTL is not always better correlated with socioeconomic data at coarser scales, however: Forbes (2013) finds that in the United States, SOL and GDP are more strongly correlated at the metropolitan than state scale. To better understand scale effects, Forbes (2013) recommends examining the processes driving relationships between NTL and socioeconomic data at varying scales and across time rather than focusing on correlations at single scales within single time periods.

4. Applications of multitemporal NTL imagery for socioeconomic dynamics

4.1. Quantitative meta-analysis

We review peer-reviewed journal papers identified by searching ISI Web of Science's archive of all journals using the terms "DMSP-OLS," "VIIRS," or "DNB" and "time-series" or "multitemporal" or "panel". After inspecting the papers and excluding those that did not concern

socioeconomic variables while adding others found on Google Scholar, mostly in the field of economics, which did not appear in the ISI results, in total, 63 peer-reviewed studies between January 2004 and July 2016 utilizing multitemporal OLS and/or VIIRS imagery to assess socioeconomic changes were identified. These largely examine urbanization, population growth, and economic growth at a range of time steps between 1992 and 2014. We entered the qualitative and quantitative information for each publication into a database containing 15 fields. Table 2 includes approximately a quarter of these studies as representative examples of research to date.

Geographically, China dominates the literature (Fig. 3). Twenty out of the 63 studies we identified focus exclusively on the country (Cao et al., 2014; Gao et al., 2015; Fan et al., 2014; He et al., 2012, He et al., 2006; Jiang et al., 2012; Li et al., 2013c; Liang et al., 2014; Liu et al., 2014, 2012, 2011; Ma et al., 2012; Su et al., 2015; Tan, 2015; Tian et al., 2014; Xiao et al., 2014; Xu et al., 2015, Xu et al., 2014; Yi et al., 2014; Zhao et al., 2016), while Sutton et al. (2007) also use it as one of their four case studies. It is important to point out that the strong focus on China may be promoting overconfidence in the ability of NTL to serve as a proxy for socioeconomic dynamics in other areas. Fifteen studies examine multitemporal NTL on a global scale (Alesina et al., 2016; Cauwels et al., 2014; Ceola et al., 2015; Chen and Nordhaus, 2011; Doll and Pachauri, 2010; Frolking et al., 2013; Geldmann et al., 2014; Henderson et al., 2012; Hodler and Raschky, 2014; Li et al., 2013b; Liu et al., 2015a; Keola et al., 2015; Nordhaus and Chen, 2015; Zhang and Seto, 2013, Zhang and Seto, 2011), while an additional two look at a large (>39) number of countries mostly in the developing world (Gennaioli et al., 2014; Weidmann and Schutte, 2016). Six studies either confine their analysis to the contiguous U.S. or use it as one of their main case studies (Cao et al., 2013; Forbes, 2013; Román and Stokes, 2014; Sutton et al., 2007; Zhang et al., 2014; Zhang and Seto, 2011). Africa tends to be the purview of economists, for the region has been relatively unstudied within their field due to the paucity of economic data (Chen and Nordhaus, 2015; Michalopoulos and Papaioannou, 2014, 2013; Rohner et al., 2013). Reflecting the distressed state of affairs in the Middle East, all but one (Román and Stokes, 2014) of the four studies concerning the region use NTL to examine the impacts of war (Agnew et al., 2008; Li et al., 2015; Li and Li, 2014).

Topically, 24 out of the 63 studies we identified directly concern urbanization processes, 18 focus on economic measures, and three attempt to estimate non-urban populations. The remainder covers a range of topics, which we explore in Section 4.5. More than half (13/24) of the studies on urbanization examine China, whose dynamics, as we discuss below, are not necessarily applicable to the rest of the world. This is why analyses of cities outside China, and particularly outside Asia (e.g. Álvarez-Berríos et al., 2013; Pares-Ramos et al., 2013), are necessary in order to explore whether they exhibit different relationships between NTL and socioeconomic variables. Most studies concerning economics tended to estimate change in economic output at scales ranging from the household to country level. Three others estimated regional or ethnic inequality (Xu et al., 2015; Alesina et al., 2016) or the size of the shadow economy (Tanaka and Keola, 2016).

In terms of NTL data, 48/63 of studies explicitly state that they use OLS V4 composites, with 43 of those using the stable lights product. The other five did not state which type they used. Only four multitemporal studies were published prior to the release of the full multi-year OLS V4 product around 2007 (Filho et al., 2004; He et al., 2006; Kohiyama et al., 2004; Sutton et al., 2007), and only one study used the OLS V2 stable lights composites (Doll and Pachauri, 2010). Prior to 2007, most NTL studies were cross-sectional. This distinction is important because the relationship between, for instance, population and NTL can be very different in the cross-section versus the panel, as

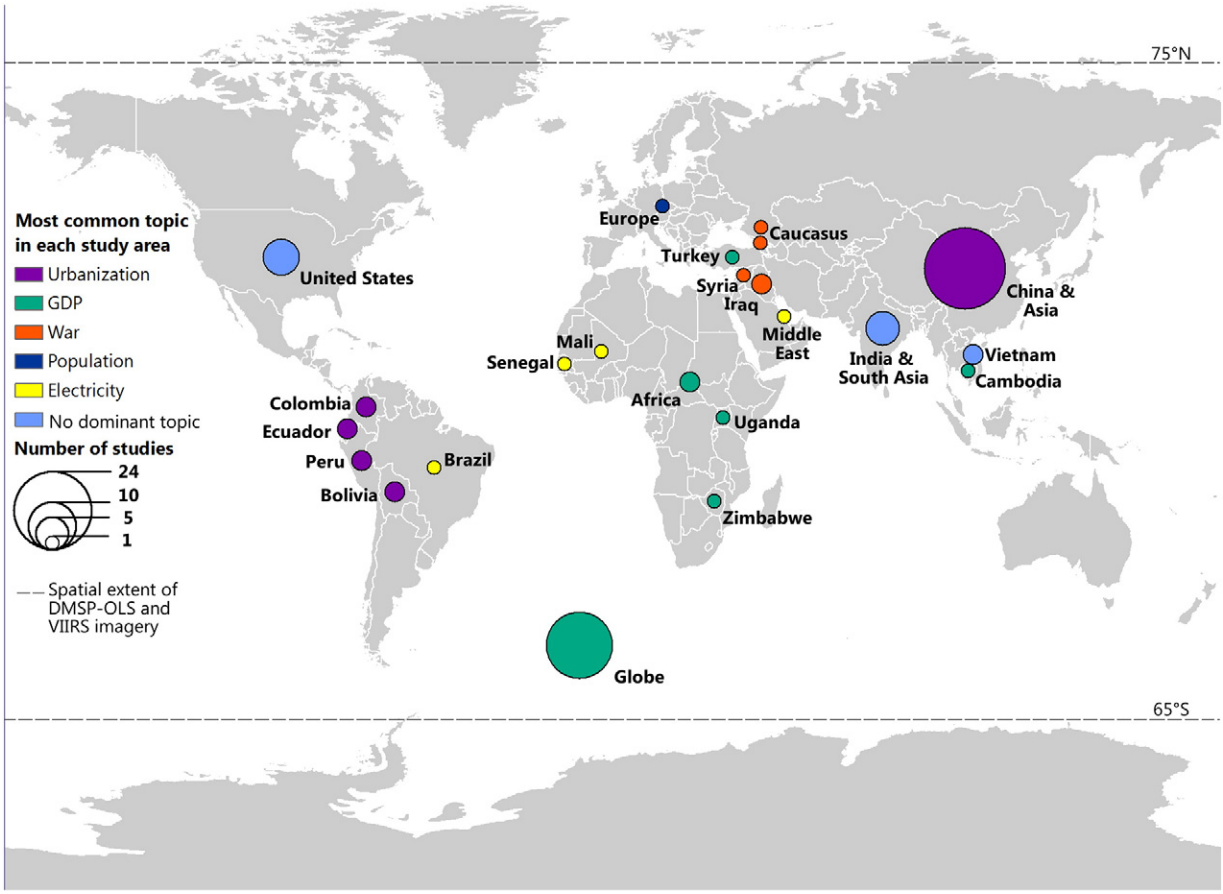

Fig. 3. Map of all identified multitemporal DMSP-OLS and VIIRS studies symbolized by most common topics.

we discuss in Section 4.4. OLS V4 data were used in 22/24 of the studies on urbanization (the remaining two did not specify the version of OLS data used) and in most studies on economic growth, although some in the latter area use other datasets like the OLS Global Radiance Calibrated Products alone (Xu et al., 2015) or in addition to OLS V4 composites (Weidmann and Schutte, 2016). Only three studies using multitemporal VIIRS data were identified (Cao et al., 2013; Xi et al., 2015; Román and Stokes, 2014), as this research still appears to be in the exploratory phase.

Another distinction among studies is the choice of using logged or unlogged units. While most NTL studies by economists use logged variables, remote sensing scientists do so less frequently. Whereas a linear relationship between two logged variables (a log-linear relationship) implies that a 10% increase in one is associated with a fixed percentage increase in another, a linear relationship between unlogged variables implies that a fixed absolute increase in one is associated with a fixed absolute increase in the other. This can be problematic when there are large outliers that might skew the relationship, and indeed the distributions for NTL, GDP, and population by country are often positively skewed. Finally, some studies demonstrate a relationship between NTL and a socioeconomic variable (e.g. Ma et al., 2012; Sutton et al., 2007; Zhang and Seto, 2013), while others take a demonstrated relationship and then use NTL to predict that variable in a different place or time with poor or non-existent records. Henderson et al. (2012), for instance, provide updated estimates of GDP for certain countries with poor economic statistics. With these issues in mind, by drawing on the multitemporal studies we identified and additional cross-sectional ones for context, the following section reviews advances made using NTL imagery for examining three key socioeconomic topics: urbanization, economic activity, and population.

4.2. Urbanization

Urbanization is a broad concept that encompasses urban population, urban land cover, and urban activities (Zhang and Seto, 2011). Aside from the simple fact that metropolises tend to be brightly lit, the city-centric focus of NTL research reflects an increasing concern in academia with the urban (Lees, 2002) and the dramatic growth of urban areas globally (Cohen, 2006). Early cross-sectional research demonstrated the usefulness of NTL as a proxy for urban population (Sutton, 1997; Elvidge et al., 1997a, 1997c). This has led OLS data to be used as an input in urban population models such as the Global Rural Urban Mapping Project (Balk, 2009). Illustrating the global rural-urban transition under way, between 1992 and 2009 cities experienced a greater proportional increase in brightness than small settlements (Cauwels et al., 2014). Caution is warranted, however, in assuming urban areas to always be light-emitting (Brenner and Schmid, 2014).

Zhang and Seto (2011) carry out one of the first studies of long-term urbanization dynamics at regional and global scales with OLS V4 stable lights composites. They estimate a linear relationship between change in urban population and NTL, with normalized urban population difference between 1992 and 2008 explaining approximately half of the variation in normalized SOL difference. However, since they do not intercalibrate their composites or control for fixed effects, their results do not account for the cross-sensor differences identified by Elvidge et al. (2009). In addition, their use of unlogged values may explain why excluding the outliers of Greenland and Russia (a country that has experienced significant economic upheaval and population decline since the Soviet collapse, potentially confounding typical relationships between these factors and NTL) increases the R^2 from 0.45 to 0.76. In another case, one outlier appears to influence the slope of the linear relationship between the normalized differences in population and urban area (extracted from OLS V4 annual stable lights composites) at the state level in India between 1998 and 2008, as shown in the scatterplot of Pandey et al. (2013), yet it is not investigated. In studies such as Zhang and Seto (2011), Pandey et al. (2013), and others that use regression-based analyses, more transparency in the handling of outliers would help determine whether they possibly share economic or geographic similarities that weaken the correlation between change in NTL and urbanization.

Some of the greatest changes in NTL have occurred in Asia (Small and Elvidge, 2013). From 1992 to 2009, the geographic center of the planet's NTL shifted 1000 km east, reflecting the growth of the continent's metropolises over the past two decades (Cauwels et al., 2014). A stratified random sampling scheme of NTL pixels from OLS V4 F14 stable lights data finds that a quarter of the world's rapid and moderate urbanization between 1997 and 2003 occurred in China (Zhang and Seto, 2013). China's cities attract a high degree of attention within the NTL literature on urbanization (Fan et al., 2014; Gao et al., 2015; Liu et al., 2014, Liu et al., 2012, 2011; Ma et al., 2012; Tan, 2015; Xiao et al., 2014; Xu et al., 2014). Many of these studies find strong relationships over time between change in NTL (both in terms of SOL and lit area) and change in variables such as urban population growth, urban GDP, urban area expansion, and urban electric power consumption in China's cities. However, the quantitative responses of changes in NTL to changes in these variables can differ between cities. Using 1994–2009 weighted lit areas from the OLS V4 stable lights composites for over 200 cities in China, Ma et al. (2012) determine that while the relationship between change in GDP and weighted lit area for cities like Beijing and Nanjing follows a power-law model, a linear model better describes the relationship for other cities in earlier stages of development, like Jinan and Fushun. These results suggest that rather than relying solely on linear functional forms, researchers should instead consider the diversity of responses of NTL to socioeconomic dynamics depending on an area's level of development.

On the whole, China's cities still are relatively uniform in terms of their urbanization patterns, with rapid and moderate urbanization occurring across the country (Zhang and Seto, 2013). In comparison, South American cities exhibit striking differences in spatiotemporal urban dynamics (Álvarez-Berríos et al., 2013). Ecuador and Bolivia's cities are undergoing an “intermediate” urban transition, with higher annual expansion rates of brightly lit pixels (>52–63 DN) than Peru and Colombia, whose cities are undergoing an “advanced” urban transition. Studies that simply calculate the difference in a city's total SOL miss such nuances of urban change.

The rate of change, or slope, of the relationship between urbanization and NTL also differs dramatically across cities even within a single country. In cases where NTL is used as a proxy, invariance of slope across contexts is possibly more meaningful than invariance of the coefficient of determination (R^2) even though this tends to be the more commonly reported result. Even if the R^2 is uniform across scales or contexts, a varying slope dramatically limits the use of NTL as a proxy. As an example of slopes varying within a single country, Gao et al. (2015) find that in China at national, provincial, and county levels, the compounded NTL index (generated by multiplying the average DN of all lit pixels in a region with the proportion of lit urban areas to total area in the region) increases by 1705.43, 90.52 and 72.81 units, per unit increase in the urbanization index, respectively. Values for the urbanization index are generated by adding various socioeconomic measures pertaining to urbanization.

The slope of the relationship between NTL and urbanization varies between countries, too. Zhou et al. (2015b) regress NTL growth rate from 2000 to 2010 (calculated by the change in the SOL where DN ≥ 13) against logged population in 2000 for cities in five Asian countries. India's slope is 0.37 (expressed in units of change in logged population per change in NTL growth rate), Pakistan = 2.33, Nepal = 5.53, Sri Lanka = 0.37, and Bangladesh = 1.73, yet no analysis is made of the widely varying slopes. Using OLS V4 stable lights composites from 1992 to 2012, Liu et al. (2015a) find that the average DN (among pixels whose DN > 30) of rapidly growing cities like Shanghai and Dubai increases mores per year (0.76–1.58 DN) than in sluggishly growing cities like Brussels, London, and Stockholm (0–0.08 DN). The median slope

(Theil-Sen estimator) is calculated between all pairs of observations for each city, with the resulting values ranked and classified from sluggish to rapid urbanization. For cities like London, saturation, an actual slowdown in urbanization, or some combination of the two may be the reason(s) for the negligible annual change in average DN. Persistent uncertainties regarding whether changes in observed NTL are happening on the ground or are merely sensor artifacts underscore the need for greater research in this area, which is discussed in Section 5.

Combining optical datasets or even ground-truthing NTL data with surveys and fieldwork (e.g. Amaral et al., 2006; Min et al., 2013; Min and Gaba, 2014) may improve accuracy and reveal the sources of observed light in cities. This is particularly true for the developing world, where NTL less accurately identifies urbanization than in developed countries. In India, for instance, many urban areas still lack electricity, impeding detection by OLS or VIIRS (Zhang and Seto, 2013). Generally, urbanization is less correlated with outdoor and street lighting in the developing world than in industrialized regions (Zhang and Seto, 2013). To identify urban area increase in India, Pandey et al. (2013) stack intercalibrated OLS V4 stable lights composites and SPOT vegetation NDVI data for the years 1998 and 2008. This extends the multisource image classification method developed by Cao et al. (2009), which largely improves detection of urban area over the use of simple global threshold in part by more accurately excluding vegetated areas and water pixels. Frolking et al. (2013) examine OLS data from 1999 to 2009 and compare the average DN per 11 × 11-cell grid in 100 large cities with backscatter power from NASA's SeaWinds microwave scatterometer. They find that while Indian cities are building outwards rather than upwards, causing growth in lit area, Chinese cities are expanding their material infrastructure in both height and extent, causing increased light intensity as well as growth in lit area. In this manner, further combination of OLS and VIIRS data with other remotely sensed imagery may help better attribute the causes of observed NTL across a range of development levels.

4.3. Economic growth and decline

A wealth of studies confirms a strong relationship between NTL and economic activity in a single year (Doll et al., 2006; Ebener et al., 2005; Sutton et al., 2007; Sutton and Costanza, 2002). In cross-sectional analysis, NTL tends to have a stronger relationship with GDP than population (Elvidge et al., 1997c; Zhou et al., 2015b). Across a diverse group of 21 countries, lit area and GDP follow a log-linear relationship with an R^2 of 0.97 (Elvidge et al., 1997c). The linkage of lit area and, more typically, derivatives of SOL with economic activity allows mapping and estimation of GDP from NTL at a range of scales in places where no standard accounts data exists, as exemplified by the production of the first-ever 1° × 1° global map of GDP (Doll et al., 2000). Although Sutton et al. (2007, p. 12) argue that OLS data can only crudely, if still significantly, estimate sub-national GDP due to its coarse spatial and spectral resolution, it has been used to accurately predict household-level wealth in developing countries (Weidmann and Schutte, 2016; Jean et al., 2016).

In a landmark panel study using OLS V4 stable lights composites to predict real income growth in 188 countries over 17 years, NTL and GDP are shown to exhibit a log-linear relationship (Henderson et al., 2012). Globally, the elasticity of SOL to GDP is 0.28 and highly significant. SOL explains approximately 77% of variation in GDP over time within a country (accounting for year fixed effects), although it explains only 21% of variation in GDP after the data is demeaned. Henderson et al. (2012) conclude that NTL growth is a highly useful proxy for both long-term GDP growth and short-term fluctuations and consequently offer amended GDP growth rates for countries with poor economic statistics like Burundi and Myanmar. However, their model assumes that the true relationship between logged NTL and GDP at the country level varies annually by a log-additive constant, which may not always be the case.

Several multitemporal NTL studies in economics build on the work of Henderson et al. (2012). Unlike most NTL research conducted by remote sensing scientists, economists tend to run panel regressions with sensitivity analyses and examine NTL in more unconventionally bounded areas, such as portage sites along the fall line (a geomorphological break between upload and coastal regions) of the Southeast U.S. (Bleakley and Lin, 2012) and ethno-linguistic homelands around the world (Alesina et al., 2016). Economists also employ ancillary data apart from the conventional measures of population and GDP. For instance, in a panel study using the Armed Conflicts Location Events Data and Afrobarometer survey data on trust and socioeconomic characteristics, Rohner et al. (2013) determine that NTL intensity declines following conflict in ethnically fractionalized countries. In another example, in a panel of 38,427 subnational regions from 126 countries spanning the years 1992–2009, Hodler and Raschky (2014) use information on national political leaders' birthplaces and find a 4% increase in NTL in their native region after entering office. Hodler and Raschky (2014) present this as evidence of regional favoritism, illustrating the power of combining NTL data with qualitative information to pursue economic lines of inquiry beyond GDP estimates.

Economists and remote sensing scientists working with NTL imagery appear to infrequently cite each other, but each community could benefit from learning about the other's methods. Since, in effect, NTL data opened up the field of remote sensing to economists, it would be beneficial to expand upon this interdisciplinary work (Keola et al., 2015). Keola et al. (2015) investigate the causal relationship between agriculture and NTL by mapping luminosity in OLS V4 composites against MODIS land cover product MCD12Q1 on a cell-by-cell basis from 1992 to 2009 and integrate the land cover data into the estimation model proposed by Henderson et al. (2012). Areas classified by MODIS as cropland, rice field, and vegetation emit relatively little or no light compared to urban areas. Thus, in countries where agriculture comprises more than half of the economy, the elasticity of logged NTL on logged GDP (including country- and year-fixed effects) is insignificant and only 0.03. This is below the global average elasticity of 0.28 found by Henderson et al. (2012), and far below the highly significant elasticity of 0.67 that Keola et al. (2015) calculate in non-agricultural countries, where farming comprises <10% of the economy. Even within these highly developed and urbanized countries, however, more work needs to be done to discern the relationships between NTL and the economic sectors often associated with them. Steelmaking, for instance, generally produces more light than software development (Henderson et al., 2012), even though it may contribute less overall to GDP.

The above studies illustrate the challenges with making inferences from log-linear relationships between NTL and GDP at regional and international scales. In a panel of 83 countries from 1992 to 2010, Gennaioli et al. (2014) show that differences in GDP per capita explain much of the variation within countries in NTL, as might be expected. However, actual NTL intensity per capita is 3.6% lower than predicted by regional GDP per capita in the poorest (bottom quartile) regions and 2.5% higher than predicted in the wealthiest (top quartile) regions. Further research into the causes of these prediction errors should help researchers seeking to estimate GDP from NTL to avoid overestimates in highly developed areas and underestimates in less developed areas.

As with urbanization and population, growth in economic activity receives more attention than decline in the published literature. Yet some studies do examine the latter phenomenon. In post-Soviet cities, the decline of NTL over time may be in response to economic conditions (Elvidge et al., 2005). The same may be true in Zimbabwe, where dimming NTL is associated with the severe economic contraction that occurred between 1992 and 2009. Using 500 samples of the rates of change for SOL against GDP within this period for the African nation, Li et al. (2013a) find an R^2 of 0.55 with no major outliers. NTL, however, has also dimmed in places not experiencing economic or population decline like Scandinavia, perhaps instead reflecting successful control of

light pollution (Bennie et al., 2014). Overall, Henderson et al. (2012) find that NTL responds symmetrically to both positive and negative income changes between 1998 and 2008, meaning that there is an absence of ratchet effects. Yet over shorter time periods, the dimming of NTL due to economic downturns may be lagged, leading Henderson et al. (2012) to propose that NTL data is best suited to predicting long-term growth rather than its converse: short-term decline.

Finally, despite all the existing research using NTL as a proxy for economic output, marked disagreement remains on the robustness of this relationship in developing countries. Whereas most research examines relationships between NTL and economic activity, Nordhaus and Chen (2015) focus on estimating the reliability of NTL as a proxy for national and regional economic output. In their previous research, they found that OLS stable lights composites add value as an economic proxy for countries with poor economic reporting in both cross-sectional and time-series analyses (Chen and Nordhaus, 2011). However, Nordhaus and Chen (2015) conclude that for time-series analysis, OLS data can contribute very little to estimates of changes in economic activity in any countries where data is available, differing from Henderson et al. (2012). Even in countries with poor or sparse records, Nordhaus and Chen (2015) argue that neither OLS data nor the intercalibration model is refined enough to allow accurate estimations of economic growth from multitemporal NTL imagery. The authors do find, though, that NTL data may have substantial value in cross-sectional estimates of economic output, as most of the sources of unreliability in using NTL as a proxy for single-year economic output come from uncertainties in national accounts data rather than uncertainties in the OLS data (Nordhaus and Chen, 2015). Arriving at a similar conclusion, Sutton et al. (2007) find that most estimation error in correlating NTL with economic growth tends to occur in sub-national regions with very low economic activity, implying either underreporting of GDP or an inability of OLS to detect dim lights associated with low levels of economic activity. For all of these reasons, estimating economic growth for countries with low levels of development remains a challenge with OLS data. Promisingly, VIIRS data are shown to be more strongly correlated with economic output than OLS stable lights data and at finer scales (Chen and Nordhaus, 2015). VIIRS may also improve estimates for places with low or dimly lit economic activity if it is able to detect low levels of light in places coded in DMSP-OLS data as DN = 0. Thus, the higher sensitivity and on-board calibration of VIIRS may help to obtain improved estimates of economic growth and decline from space.

4.4. Population change

Most of the world's population growth is occurring in developing countries, where population statistics often lack accuracy. This makes NTL data a potentially key source of information for estimates. Modeling population dynamics in the developing world is challenging, however, because globally, the minimum population detectable by OLS varies. Africa has a lower population density than Asia, Europe, and North America, meaning that the NTL thresholds needed to detect human activities are likely lower. Cross-sectional analysis has shown that the mean population density of unlit areas ranges from 10.05 persons/km^2 in Latin America and the Caribbean to 208.18 persons/km^2 in India (Doll and Pachauri, 2010). Population density therefore has a weaker relationship with NTL intensity than economic activity. A place with 1000 persons/km^2 will be brighter in a developed country than a developing region, although there is significant scatter in this relationship (Raupach et al., 2010). This variation complicates efforts to estimate regional or global population levels from NTL.

NTL change is largely positively correlated with population change, but this may be because population continues to grow globally. Certain areas with decreasing populations actually exhibit negative correlations with NTL change. In 90% of countries, NTL change from 1992 to 2012 moved in the same direction as change in population, along with GDP (Elvidge et al., 2014). Many of the exceptions are concentrated in the former Soviet Union and Eastern Europe, where population has decreased in a significant number of countries. These exceptions can be divided into two groups. In the first group of outliers, NTL change is positively correlated with GDP change but negatively correlated with population change (so lights stay on even as population declines). Examples of these countries with so-called "GDP-centric" NTL include Albania and Poland. In the second group of outliers, NTL change is positively correlated with population change but negatively correlated with GDP change (so lights stay on even as GDP declines). Examples of these countries with so-called "population-centric" NTL include Russia and Kazakhstan (Elvidge et al., 2014). Further confirming the unusual nature of the relationships between NTL and population in Eastern Europe, using country-level SOL derived from intercalibrated OLS V4 stable lights composites from 1992 to 2012, Archila Bustos et al. (2015) find that only 23% of significant cases of decreasing population reveal coupling with lit extent while 93% of significant cases of increasing population exhibit coupling. For instance, the former Soviet republics of Latvia, Lithuania, and Estonia show consistent increases in NTL despite decreases in population. Archila Bustos et al. (2015) conclude that the strong positive relationship found between NTL and population in single-year cross-sectional analyses (e.g. Elvidge et al., 1997c; Sutton et al., 2001) can break down when examined within a country over time. Even outside of Eastern Europe, NTL and population change are sometimes decoupled. In brightly lit urban areas in South Asia, Zhou et al. (2015a) find no correlation between the growth rates of annual population and SOL ($R^2 = 0.02$). All of these findings indicate the need for caution when predicting population change from NTL.

Despite these caveats, Ceola et al. (2015) use NTL to infer population dynamics. They determine that from 1992 to 2013, human populations have moved significantly closer to rivers around the world by calculating the changes in total and average SOL at a 1-km^2 resolution within five distance classes near streams and rivers. Yet given existing variations in average NTL per capita based on a country's level of economic development, a 5-DN pixel change along the Nile may correspond to a larger population change than a 5-DN pixel change along the Danube. Thus, even if population and NTL change are assumed to be coupled, precisely quantifying the population change remains difficult.

As with NTL-based estimates of economic activity, dark or very dim pixels can impact population estimates. Just as farming and logging do not emit high degrees of light despite contributing to GDP, many places do not emit observable light despite being inhabited. An estimated 1.5 billion people live without any access to electricity whatsoever, rendering their populations, and by corollary any changes in their numbers, largely undetectable in NTL imagery (Doll and Pachauri, 2010). Nordhaus and Chen (2015) determine that in the OLS V4 stable lights composite for the year 2000, nearly a third of 1° × 1° grid cells that actually do have population and economic output are coded as DN = 0. Russia, Canada, and Africa contain 67% of these "zero lights" cells. Although they are estimated to comprise only 0.4% of global population and economic output, the zero lights cells cover a sizeable portion of the world's landmass. Since it is unlikely that population or economic activity occurs completely without light, the zero-lights encoding may be due to the inability of OLS to resolve dim lighting. It may also be due to the stable lights composites' exclusion of areas with unstable lighting, which is common in rural villages in the developed world with low power loads (Min and Gaba, 2014).

VIIRS may help to more accurately detect and estimate populations in both developed and developing regions thanks to its lack of saturation and lower detection limit. Early cross-sectional research demonstrates this potential. Along a 100-km latitudinal transect centered on Beijing, VIIRS-measured radiance also shows a slightly stronger response to urban population than OLS stable lights ($R^2 = 0.89$ versus $R^2 = 0.83$, respectively), with the ability to detect variations in the urban-rural transition zone, too (Ma et al., 2014c). At the 1° × 1° grid-cell scale in Africa, the relationship between NTL intensity and population has an R^2 of 0.59 for a two-month VIIRS composite from 2012

compared to 0.27 for an OLS F18 2010 stable lights composite (Chen and Nordhaus, 2015). More time must pass before a substantial record of VIIRS imagery is built up to examine annual population changes, although the potential for decoupling between NTL and population change may still affect reliable estimates of population change. Regardless, based on observed publication trends following the release of the OLS V4 stable lights product from 1992 to 2013, we venture that the creation and public release of annual VIIRS stable lights composites would assist in this regard. Already, the VIIRS NTL 2012 composite serves as an input to the WorldPop global population product (Stevens et al., 2015).

4.5. Additional socioeconomic dynamics

Multitemporal NTL data are employed to study a wide range of additional socioeconomic dynamics. Regional inequality (Xu et al., 2015; Zhou et al., 2015a), electricity consumption and access patterns (Cao et al., 2013, Cao and Bai, 2014; Chand et al., 2009; Doll and Pachauri, 2010; Filho et al., 2004; He et al., 2012; Min and Gaba, 2014; Min et al., 2013), power outages due to natural disasters (Cao et al., 2013; Kohiyama et al., 2004; Molthan and Jedlovec, 2013), increases in freight traffic (Shi et al., 2015; Tian et al., 2014), human impacts on the environment (Geldman et al., 2014; Liu et al., 2014), steel stock use (Liang et al., 2014), and the effects of armed conflict (Agnew et al., 2008; Li et al., 2013b; Witmer and O'Loughlin, 2011; Xi et al., 2015) constitute several examples. Multitemporal NTL can also be harnessed to show how an expanding human footprint can impact conservation (Venter et al., 2016) or protected areas (Gaston et al., 2015; Geldmann et al., 2014).

Despite the low spatial resolution of OLS, Witmer and O'Loughlin (2011) are able to associate NTL with large, long-lasting fires and refugee movements in the war-torn Caucasus. This may suggest that with VIIRS, finer scale movements of refugees such as from Syria to Europe may be detectable from space. The Syrian civil war has created a number of opportunities for using multitemporal VIIRS data for humanitarian monitoring. Li and Li (2014) find a 74% and 73% decrease in Syria's SOL and lit area, respectively, between March 2011 and February 2014. They conclude that change in SOL explains 52% of the variation in the number of internally displaced persons in all of the country's provincial regions. Further to their study, Fig. 4 visualizes the dramatic decline in NTL in Syria between 2014 and 2016 along a highway controlled by ISIS and brightening across the border in southern Turkey, where hundreds of thousands of refugees have fled. Painting a happier picture, Román and Stokes (2014) associate fluctuations in radiance in cities in the United States and Middle East with neighborhood holiday lighting patterns, suggesting that VIIRS data could be used to eventually help generate finely tailored energy conservation strategies. Thus, even more than OLS, VIIRS can inform studies of socioeconomic dynamics from the neighborhood to the global scale.

5. Future directions

5.1. Understanding the causes of observed light

While NTL data are a valuable tool for studying development, they are subject to a number of basic limitations. NTL depends on economic activity, population density, lighting type, and lighting regulations, all of which vary between countries, subnational regions, and even within cities. This variation makes comparisons across space and time challenging and presents a barrier to understanding the precise relationships between changes in NTL and socioeconomic dynamics. Thus, more systematic analysis of the causes of observed light across regions and developmental contexts is required. It is well understood that NTL is broadly correlated with urbanization, population, and economic output in international comparisons and at the subnational level in highly developed Western countries and in fast-growing China. Yet comparatively little is known about exceptions to these relationships, particularly with regard to how their strength may vary at the subnational level in the developing world.

Further research into the emission of light (or lack thereof) may be done through 1) additional combination of OLS or VIIRS data with

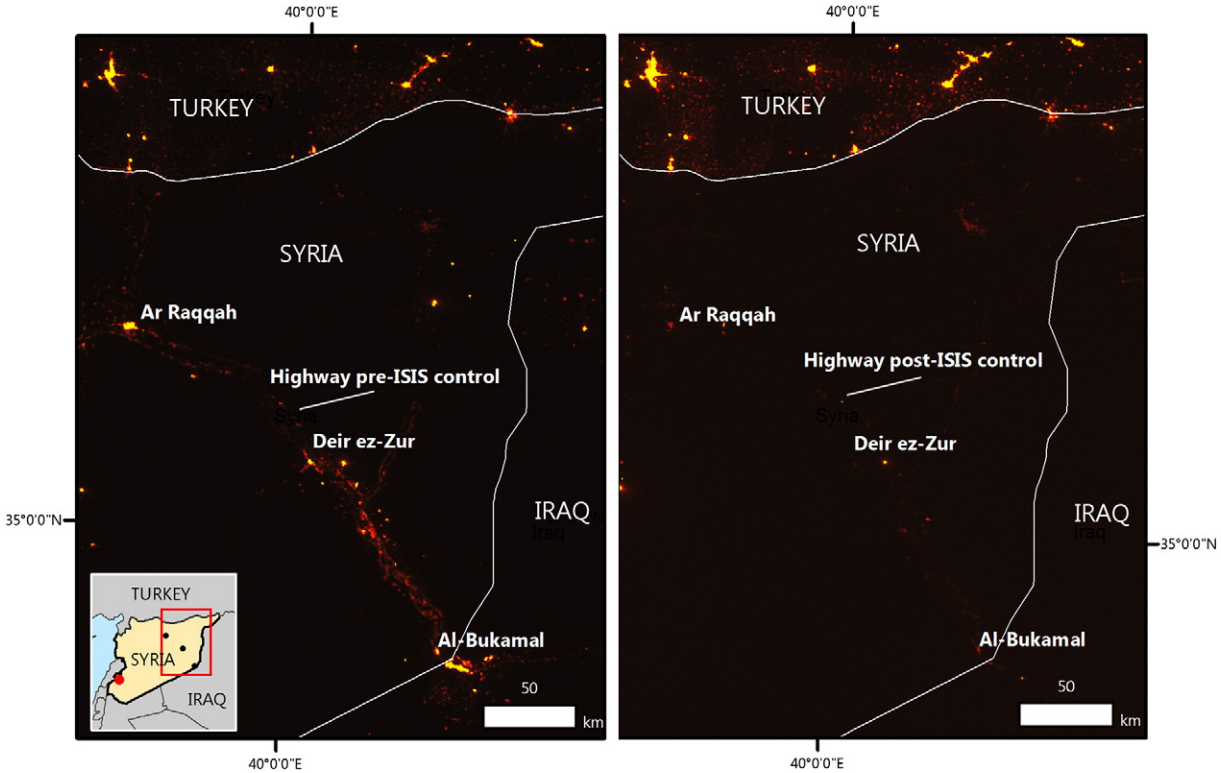

Fig. 4. Left: April 2014 monthly VIIRS composite of northeast Syria pre-ISIS control of a major highway. Right: April 2016 monthly VIIRS composite of the same area.

other remotely sensed data products; 2) statistical analyses that explore interactions between the variables influencing NTL and more closely inspect outliers; and 3) site-specific analyses through fieldwork. Although these directions have been pursued in certain studies, they have yet to be widely adopted.

First, research should consider integrating other remotely sensed datasets into NTL-based models rather than just using them for validation. Several studies, for instance, validate OLS and/or VIIRS imagery with photographs taken from the International Space Station (Elvidge et al., 2007; Levin and Duke, 2012) or Landsat data (Levin and Phinn, 2016; Castrence et al., 2014; Shi et al., 2014; Small et al., 2005; Zhang and Seto, 2011). But rather than just using non-NTL imagery for examining the "accuracy" of NTL, more insight into the factors driving observed lights may come from combining both datasets into the same model. Drawing on how Keola et al. (2015) use MODIS imagery to quantify the differences in emissivity between typically dim forests and farmland and bright, urbanized areas, more first-order research is necessary to systematically understand the reasons for differences in NTL across economic sectors and regions. Incorporation of other remotely sensed data, like AVHRR, Landsat, MODIS, SPOT VEGETATION, MODIS, or Sentinel-2 could also address how land cover can also affect NTL. The same amount of NTL, for instance, may be less visible when emitted from a forest than a grassland or desert, yet little work has investigated the effects of ground cover on NTL. Lastly, researchers can borrow from methods more typically used by remote sensing scientists to study physical processes, similar to how Small and Elvidge (2013) employ the empirical orthogonal function (EOF), often used in oceanography and meteorology, to examine decadal changes in NTL in Asia. This approach provides a robust and straightforward way to characterize spatial and temporal patterns and does not require the assumption of temporal change taking specific functional forms, such as linear or sinusoidal. More creativity in modeling strategies may be productive for multitemporal analysis.

Second, further exploration of heterogeneity and change in the relationships between NTL and development indicators may more clearly demonstrate how social and economic variables interact to produce lights. This approach would provide an alternative to the current emphasis in much of the literature on explaining variation in the level of light output, as reported in R^2 and goodness of fit statistics. It would also draw on early work like Tobler (1969), who confirmed with satellite imagery that the relationship between a settlement's size and its population differs by country. While this relationship maintains a generally similar R^2 across countries, the correlation of proportionality varies from one country to the next. Societal factors clearly influence patterns of lights separately from GDP and population: for instance, the SOL of an American town of 10,000 inhabitants tends to be three times larger than an equivalent German town, while an American city of 100,000 inhabitants has five times more SOL (Kyba et al., 2015). This may be because German policy tends to be conservative in its use of public and outdoor lighting; the country does not widely illuminate its highway network, for instance. Although sociocultural causes for differences in lights remain understudied, attempts to predict GDP, population, or other variables from NTL data without taking such factors into consideration may lead to inaccurate results.

Additionally, examinations of interactions, which are when the effect of one independent variable depends on the type or level of another independent variable, could prove useful. Rohner et al. (2013), for instance, model interactions to show that for African countries, conflict only negatively impacts development (proxied by decreasing NTL) in those that are ethnically fractionalized. Another example of the types of questions that could benefit from interaction analysis is whether the relationship between NTL and fixed capital investment (FCI), generally defined as the value of new construction, expansion, or renovation to physical capital (i.e. buildings and machinery), depends on a region's dominant economy. This question is motivated by Fig. 5, which shows how in Russia, certain oil-producing federal subjects (the top-level political divisions within Russia) have unusually low levels of SOL relative to FCI, regardless of whether the variables are logged. Possibly, an over-exclusion of NTL values due to high levels of gas flaring in the Yamalo-Nenets Autonomous Okrug (YNAO), Khanty-Mansiysk, and part of Tyumen results in their low levels of NTL. Yet it may be worth investigating whether some other variable that could be interacted with FCI, like size of the oil industry, is driving their unusual relationships, too.

More attention to outliers is also warranted as they may be theoretically and empirically meaningful, but are frequently omitted from analyses to improve the overall fit of statistical models. Logging can also obscure outliers, which is why data should be carefully inspected and outliers presented before logging variables. Fig. 5 also illustrates how outliers can become obscured even though their atypical relationships with NTL that are visible before logging may be worth investigating. Leaving aside the three aforementioned oil-producing federal subjects and Moscow and St. Petersburg, which may be outliers because they are geographically small, highly saturated, and highly urbanized federal districts, one outlier still remains: Krasnodar, host of the 2014 Winter Olympics in Sochi and one of the most corrupt regions in Russia (Panifilova, 2016). If the data had only been inspected after logging, then the relatively low amount of NTL that Krasnodar emits per ruble of FCI compared to most of Russia's other regions, an insight which may merit further inquiry, may not have been as apparent.

A third way to better understand the causes of observed light is through site-specific analyses, namely fieldwork. To illustrate with a preliminary demonstration, in March 2016, we conducted ethnographic fieldwork on post-Soviet transportation infrastructure development in the Russian Far East. While no field measurements of light pollution were made, it is possible to pair qualitative observations made during our fieldwork with a map of the region showing the change between OLS V4 stable lights in 1992 and 2012 (both intercalibrated following Elvidge et al. (2009)) (Fig. 6). Over these two decades, the Trans-Siberian Railway, large cities like Khabarovsk, and small settlements decline. But somewhat uniquely, the city of Blagoveshchensk, which sits directly on the Amur River border across from Heihe, China, has brightened, perhaps thanks to its close cross-border ties with its booming East Asian neighbor. Khabarovsk, which sits 30 km away from the border, has experienced no such increase in NTL. Fieldwork in Blagoveshchensk revealed Chinese and Russians engaging in significant amounts of cross-border tourism. Many Chinese merchants have also opened businesses in Blagoveshchensk, while this appeared less common in Khabarovsk. These findings in Blagoveshchensk may represent an exception to Pinkovskiy (2013), who finds that both NTL per capita and its growth rate decrease discontinuously when a border is crossed from a faster-growing to a slower-growing country. They should also encourage further work that takes advantage of the boundless nature of NTL data by examining imagery outside of national frameworks and looking, for instance, for the most rapidly growing cross-border regions or ecosystems in the world.

Finally, at the neighborhood scale, differences in NTL match differences in urban development observed during fieldwork in Vladivostok, a city on Russia's Pacific Coast that has received numerous investments in infrastructure and a new university under President Vladimir Putin. Whereas the central business district is flourishing with a waterfront revitalization project and new condominiums, obsolete and abandoned buildings litter the landscapes of outlying micro-districts (*mikrorayon*) such as Podnozhye. In short, combining NTL data with fieldwork opens the door to collaborations with social scientists like anthropologists, political scientists, and geographers. Since NTL imagery provides an important quantitative proxy for socioeconomic activity, involving social scientists beyond economists to contribute qualitative observations regarding the potential causes of observed light could prove enlightening.

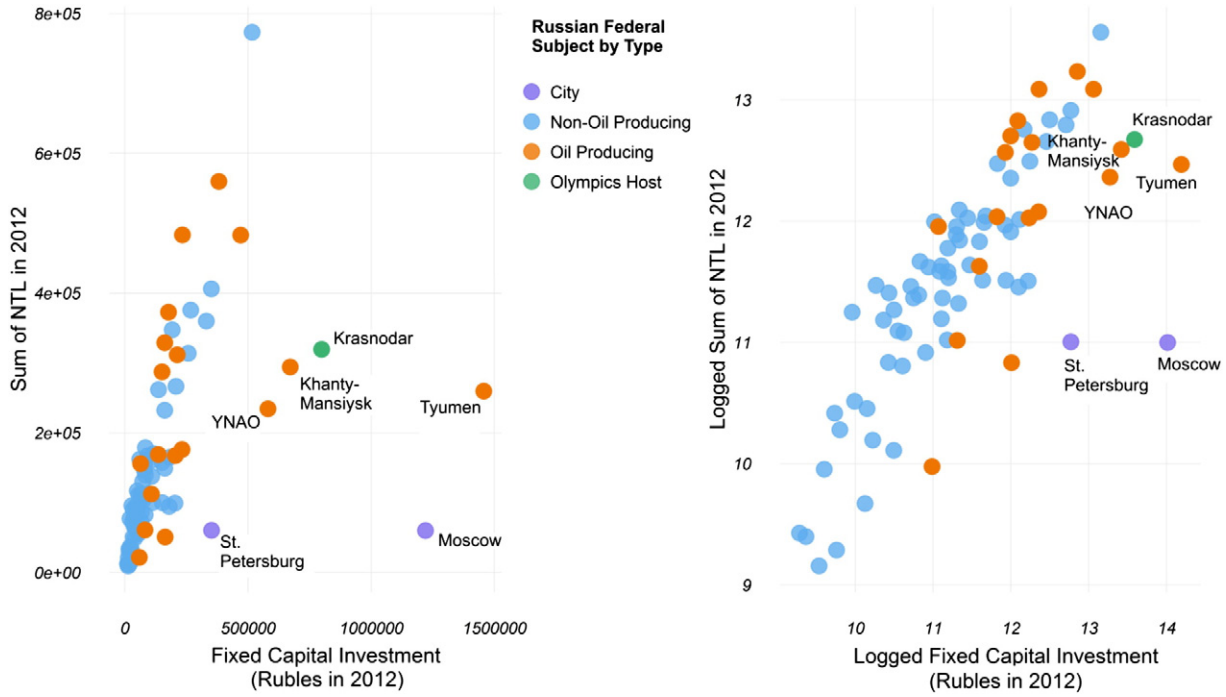

Fig. 5. Fixed capital investment versus SOL in 2012 for Russia's federal subjects, in unlogged and logged forms. Federal districts are divided into two main categories: oil producing and non-oil producing in 2011. The outliers of Moscow, St. Petersburg, and Krasnodar are highlighted for reasons discussed in the text. Federal districts data: Global Administrative Unit Layers 2015, Food and Agricultural Organization, 2015. Lights data: Zonal sums calculated in ArcGIS from OLS V4 Stable Lights composites with gas flares subtracted. Oil production data: RIA Novosti, 2012. Fixed capital investment data: Russian Federal State Statistics Service.

5.2. VIIRS: future topics, regions, and time steps

A few key topical, regional, and temporal areas of research to pursue that leverage VIIRS' enhanced capabilities are infrastructure growth, the Arctic, and sub-annual activities. First, topically, if predictions that humans will build more infrastructure in the next four decades than they have in the past four millennia (Khanna, 2016) are to be believed, VIIRS data are well-suited to track and quantify its associated light emissions. With its coarse resolution, OLS data can be used to model the expansion of transportation corridors like highways and railways (Liang et al., 2014). But VIIRS imagery can actually reveal the fine-scale socioeconomic impacts of these infrastructures, such as CO_2 emissions along highways (Ou et al., 2015). While Elvidge et al. (2014) encourage using multitemporal NTL for infrastructure mapping, more intriguing might be to use NTL to monitor and predict the intensity and social, economic, and environmental impacts of its use. Especially if paired with GIS-based network models (e.g. Kotavaara et al., 2011), such research could help quantify the effects of the networked infrastructure developments that underlie urbanization processes (Graham and Marvin, 2001).

Spatially, what one might call one of the "last frontiers" for NTL research is applying VIIRS imagery to remote and inaccessible areas like the Arctic, Amazon and the high seas. Although OLS can capture data during the polar night, at latitudes above the Arctic Circle, these data are subject to aurora and significant year-to-year differences in resolved light owing to changing snow cover (Ebener et al., 2005; Henderson et al., 2012). Countries at high latitudes like Canada, Sweden, Norway, Finland, and Iceland also exhibit unusually high levels of lighting relative to their populations (Elvidge et al., 2001). Researchers employing VIIRS imagery still have to contend with these complications, but the sensor more accurately resolves light-emitting activities in the circumpolar north than OLS (Straka et al., 2015). Henderson et al. (2012) note that only 0.036% of the world lives in the Arctic, but as economic activities increase in the warming region, VIIRS may provide insight into the region's development. Finally, the various advances of VIIRS combined with its cost-free nature can empower polar end-users of NTL data in potentially life-saving ways. Straka et al. (2015) demonstrate how VIIRS imagery was used in near-real time to rescue an imperiled crab fishing boat off Alaska. From this vantage point, VIIRS offers new opportunities for knowledge production and practical applications in the Arctic.

Finally, temporally, the cost-free nature of DNB imagery at daily and monthly time steps opens up numerous areas for research. While cloud cover still remains an issue in daily imagery, several studies already use VIIRS data to illustrate monthly and seasonal changes in anthropogenic light-emitting activities, such as holiday lighting (Román and Stokes, 2014) and passenger traffic and aircraft movement at airports (Ma et al., 2014c). VIIRS data could also be used to detect light-emitting activities of short duration but potentially high social or environmental impacts, like unauthorized steel factories, which have been documented on the ground in China (Hilaire, 2016), or illegal fishing. Liu et al. (2015b) demonstrate how nightly VIIRS imagery can detect light-emitting squid and fishing ships and suggest that examining the NTL data against vessel monitoring system (VMS) records could reveal ships that are illegally fishing. Such law-breaking ships would emit NTL, but not a VMS signal. As with many remotely sensed datasets, the geopolitical ramifications of using this imagery for revealing clandestine or illicit activities are potentially serious (Gleason and Hamdan, 2015). Given these challenges, scientists should carefully consider but not shy away from the opportunity to use NTL data to monitor short-duration activities in vulnerable areas from war zones to the high seas.

6. Concluding remarks

Multitemporal OLS and VIIRS data allow for globally consistent studies of socioeconomic dynamics such as urbanization, population, and economic activity. With proper corrections for temporal differences (e.g. sensor intercalibration or controlling for year-fixed effects) and attention to saturation and blooming, multitemporal OLS data can provide a reasonable proxy for growth in these parameters. Declining urbanization, population, or economic activity appears more challenging to approximate, as lights do not always turn off when a place's population or GDP shrinks. Thus, future research should continue to investigate

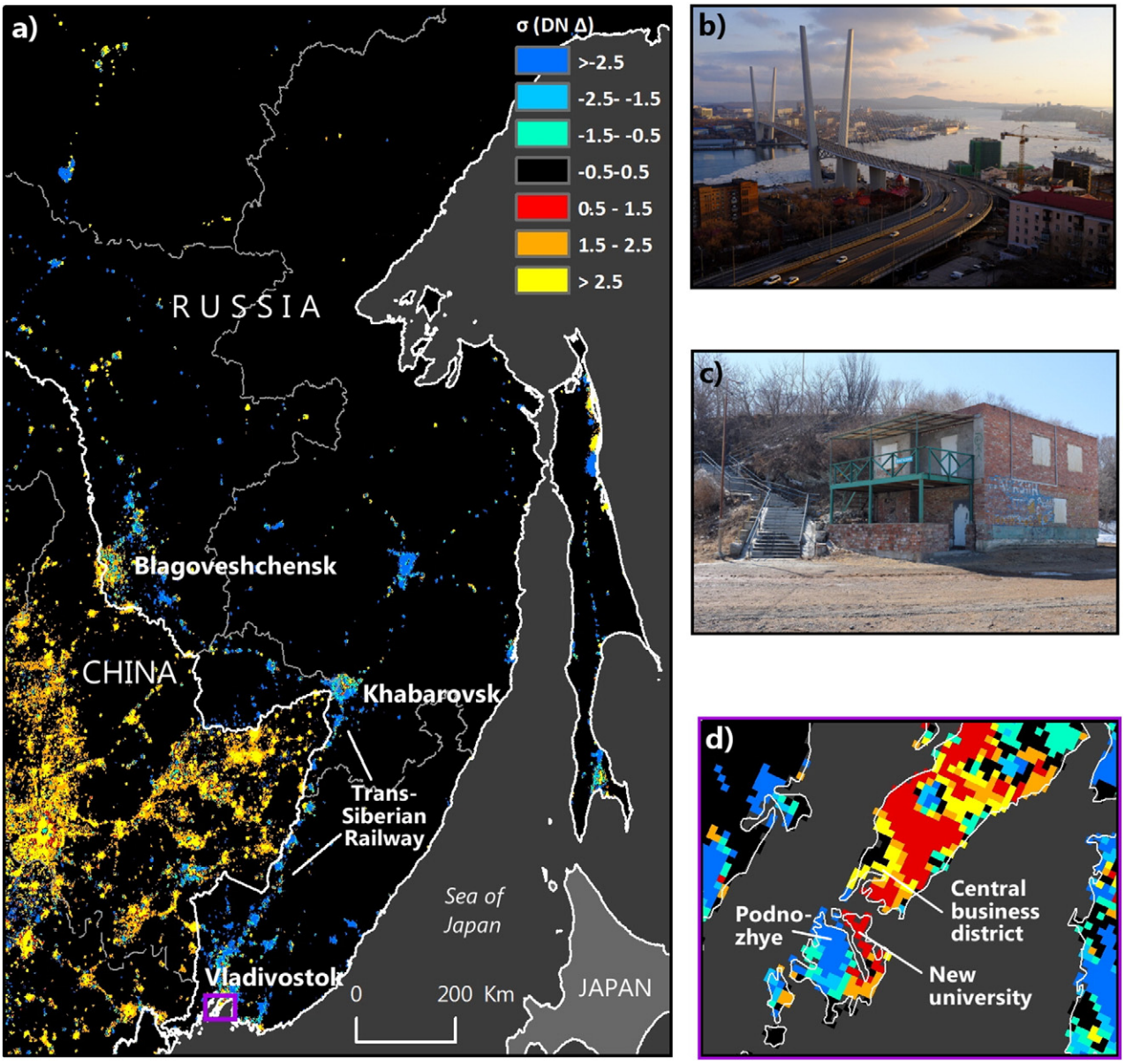

Fig. 6. Regional change detection map over the Russian Far East and Northeast China, 1992–2012, and inset map over Vladivostok, with corresponding field photographs. a) Change detection map over the Russian Far East and Northeast China, 1992–2012. b) Spanning from Vladivostok's central business district, the new Zolotoy Bridge leads towards the new university. c) An abandoned store at the disused waterfront in Podnozhye. d) Inset map of Vladivostok.

the actual causes of observed light and also attempt to determine why certain places, features, and activities remain or become dark. Future research would also benefit from integrating other remotely sensed data products with NTL imagery into the same model, more robust statistical analyses that examine interactions and outliers, and field studies and interdisciplinary collaborations.

With its dramatically enhanced spatial and radiometric resolutions, VIIRS provides a much improved view of the Earth at night compared to OLS. Saturation and blooming are significantly reduced, while measurement of actual radiance and on-board calibration facilitate accurate comparisons of NTL changes over time. The sensor's ability to detect low levels of light may also enhance the accuracy of estimates of population and economic activity in developing countries. The free distribution of daily and nightly VIIRS data and NOAA's production of monthly composites better position researchers to uncover relationships between NTL and various socioeconomic dynamics across finer temporal scales than with OLS data, too. Building on preliminary efforts to integrate OLS and VIIRS data to extend the record of comparable NTL imagery (Shao et al., 2014) would also be valuable for multitemporal studies. With OLS, VIIRS, and its forthcoming successor JPSS-1, the tools now exist to directly study and monitor anthropogenic activities once hidden by cover of night.

References

Agnew, J., Gillespie, T.W., Gonzalez, J., Min, B., 2008. Baghdad nights: evaluating the US military "surge" using nighttime light signatures. Environ. Plan. A 40:2285–2295. http://dx.doi.org/10.1068/a41200.

Alesina, A., Michalopoulos, S., Papaioannou, E., 2016. Ethnic inequality. J. Polit. Econ. 124: 428–488. http://dx.doi.org/10.1086/685300.

Álvarez-Berríos, N.L., Parés-Ramos, I.K., Aide, T.M., 2013. Contrasting patterns of urban expansion in Colombia, Ecuador, Peru, and Bolivia between 1992 and 2009. Ambio 42: 29–40. http://dx.doi.org/10.1007/s13280-012-0344-8.

Amaral, S., Monteiro, A.M., Câmara, G., Quintanilha, J.A., 2006. DMSP/OLS night-time light imagery for urban population estimates in the Brazilian Amazon. Int. J. Remote Sens. 27 (5), 855–870.

Archila Bustos, M.F., Hall, O., Andersson, M., 2015. Nighttime lights and population changes in Europe 1992–2012. Ambio 44:653–665. http://dx.doi.org/10.1007/s13280-015-0646-8.

Balk, D., 2009. More than a name: why is global urban population mapping a GRUMPy proposition? In: Gamba, Paolo, Herold, Martin (Eds.), Global Mapping of Human

Settlement: Experiences, Datasets, and Prospects. CRC Press, Boca Raton:pp. 145–161 http://dx.doi.org/10.1201/9781420083408-c7.
Baugh, K., Elvidge, C.D., Ghosh, T., Ziskin, D., 2010. Development of a 2009 stable lights product using DMSP-OLS data. Proc. Asia-Pacific Adv. Netw. 30:114–130. http://dx.doi.org/10.7125/APAN.30.17.
Bennie, J., Davies, T.W., Duffy, J.P., Inger, R., Gaston, K.J., 2014. Contrasting trends in light pollution across Europe based on satellite observed night time lights. Sci. Rep. 4: 1–6. http://dx.doi.org/10.1038/srep03789.
Bleakley, H., Lin, J., 2012. Portage and path dependence. Q. J. Econ. 127:587–644. http://dx.doi.org/10.1093/qje/qjs011.
Brenner, N., Schmid, C., 2014. The "Urban Age" in question. Int. J. Urban Reg. Res. 38: 731–755. http://dx.doi.org/10.1111/1468-2427.12115.
Cahoon, D.R., Stocks, B.J., Levine, J.S., Cofer, W.R.I., O'Neill, K.P., 1992. Seasonal distribution of African savanna fires. Nature 359, 812–815.
Cao, C., Bai, Y., 2014. Quantitative analysis of VIIRS DNB nightlight point source for light power estimation and stability monitoring. Remote Sens. 6:11915–11935. http://dx.doi.org/10.3390/rs61211915.
Cao, X., Chen, J., Imura, H., Higashi, O., 2009. A SVM-based method to extract urban areas from DMSP-OLS and SPOT VGT data. Remote Sens. Environ. 113:2205–2209. http://dx.doi.org/10.1016/j.rse.2009.06.001.
Cao, C., Shao, X., Uprety, S., 2013. Detecting light outages after severe summer storms using the S-NPP/VIIRS Day/Night Band radiances. IEEE Geosci. Remote Sens. Lett. 10:1582–1586. http://dx.doi.org/10.1109/LGRS.2013.2262258.
Cao, X., Wang, J., Chen, J., Shi, F., 2014. Spatialization of electricity consumption of China using saturation-corrected DMSP-OLS data. Int. J. Appl. Earth Obs. Geoinf. 28, 193–200.
Castrence, M., Nong, D., Tran, C., Young, L., Fox, J., 2014. Mapping urban transitions using multi-temporal Landsat and DMSP-OLS night-time lights imagery of the Red River Delta in Vietnam. Land 3:148–166. http://dx.doi.org/10.3390/land3010148.
Cauwels, P., Pestalozzi, N., Sornette, D., 2014. Dynamics and spatial distribution of global nighttime lights. EPJ Data Sci. 3:1–26. http://dx.doi.org/10.1140/epjds19.
Ceola, S., Laio, F., Montanari, A., 2015. Human impacted waters: new perspectives from global high resolution monitoring. Water Resour. Res. 51:7064–7079. http://dx.doi.org/10.1002/2015WR017482.
Chand, T.R.K., Badarinath, K.V.S., Elvidge, C.D., Tuttle, B.T., 2009. Spatial characterization of electrical power consumption patterns over India using temporal DMSP-OLS night-time satellite data. Int. J. Remote Sens. 30:647–661. http://dx.doi.org/10.1080/01431160802345685.
Chen, X., Nordhaus, W.D., 2011. Using luminosity data as a proxy for economic statistics. Proc. Natl. Acad. Sci. 108:8589–8594. http://dx.doi.org/10.1073/pnas.1017031108.
Chen, X., Nordhaus, W.D., 2015. A test of the new VIIRS lights data set: population and economic output in Africa. Remote Sens. 7:4937–4947. http://dx.doi.org/10.3390/rs70404937.
Cinzano, P., Falchi, F., Elvidge, C.D., Baugh, K.E., 2000. The artificial night sky brightness mapped from DMSP operational linescan system measurements. Mon. Not. R. Astron. Soc. 318:641–657. http://dx.doi.org/10.1046/j.1365-8711.2000.03562.x.
Cohen, B., 2006. Urbanization in developing countries: current trends, future projections, and key challenges for sustainability. Technol. Soc. 28:63–80. http://dx.doi.org/10.1016/j.techsoc.2005.10.005.
Croft, T., 1978. Nighttime images of the earth from space. Sci. Am. 239, 86–98.
Doll, C.N., 2008. CIESIN thematic guide to night-time light remote sensing and its applications. Center for International Earth Science Information Network of Columbia University, Palisades, NY.
Doll, C.N.H., Pachauri, S., 2010. Estimating rural populations without access to electricity in developing countries through night-time light satellite imagery. Energ Policy 38: 5661–5670. http://dx.doi.org/10.1016/j.enpol.2010.05.014.
Doll, C.N.H., Muller, J., Elvidge, C.D., 2000. Night-time imagery as a tool for global mapping of socioeconomic parameters and greenhouse gas emissions. Ambio 29:157–162. http://dx.doi.org/10.1579/0044-7447-29.3.157.
Doll, C.N.H., Muller, J.-P., Morley, J.G., 2006. Mapping regional economic activity from night-time light satellite imagery. Ecol. Econ. 57:75–92. http://dx.doi.org/10.1016/j.ecolecon.2005.03.007.
Ebener, S., Murray, C., Tandon, A., Elvidge, C., 2005. From wealth to health: modelling the distribution of income per capita at the sub-national level using night-time light imagery. Int. J. Health Geogr. 4:1–17. http://dx.doi.org/10.1186/1476-072X-4-5.
Elvidge, C.D., Baugh, K.E., Kihn, E.A., Kroehl, H.W., Davis, E.R., 1997a. Mapping city lights with nighttime data from the DMSP operational linescan system. Photogramm. Eng. Remote. Sens. 63, 727–734.
Elvidge, C.D., Baugh, K.E., Hobson, V.R., Kihn, E., Kroehl, H.W., Davis, E.R., Coceros, D., 1997b. Satellite inventory of human settlements using nocturnal radiation emissions: a contribution for the global tool chest. Glob. Chang. Biol. 3, 387–395.
Elvidge, C.D., Baugh, K.E., Kihn, E.A., Kroehl, H.W., Davis, E.R., Davis, C.W., 1997c. Relation between satellite observed visible-near infrared emissions, population, economic activity and electric power consumption. Int. J. Remote Sens. 18:1373–1379. http://dx.doi.org/10.1080/014311697218485.
Elvidge, C.D., Baugh, K.E., Dietz, J.B., Bland, T., Sutton, P.C., Kroehl, H.W., 1999. Radiance calibration of DMSP-OLS low-light imaging data of human settlements. Remote Sens. Environ. 68:77–88. http://dx.doi.org/10.1016/S0034-4257(98)00098-4.
Elvidge, C.D., Imhoff, M.L., Baugh, K.E., Hobson, V.R., Nelson, I., Safran, J., Dietz, J.B., Tuttle, B.T., 2001. Night-time lights of the world: 1994–1995. ISPRS J. Photogramm. Remote Sens. 56:81–99. http://dx.doi.org/10.1016/S0924-2716(01)00040-5.
Elvidge, C.D., Baugh, K.E., Safran, J., Tuttle, B.T., Howard Ara, T., Hayes, P.J., Jantzen, J., Erwin, E.H., 2005. Preliminary results from nighttime lights change detection. Int. Arch. Photogramm. Remote. Sens. Spat. Inf. Sci. 36, 14–16.
Elvidge, C.D., Cinzano, P., Pettit, D.R., Arvesen, J., Sutton, P., Small, C., Nemani, R., Longcore, T., Rich, C., Safran, J., Weeks, J., Ebener, S., 2007. The Nightsat mission concept. Int. J. Remote Sens. 28:2645–2670. http://dx.doi.org/10.1080/01431160600981525.
Elvidge, C.D., Ziskin, D., Baugh, K.E., Tuttle, B.T., Ghosh, T., Pack, D.W., Erwin, E.H., Zhizhin, M., 2009. A fifteen year record of global natural gas flaring derived from satellite data. Energy 2:595–622. http://dx.doi.org/10.3390/en20300595.
Elvidge, C.D., Baugh, K., Zhizhin, M., Hsu, F.C., 2013a. Why VIIRS data are superior to DMSP for mapping nighttime lights. Proc. Asia-Pacific Adv. Netw. 35:62–69. http://dx.doi.org/10.7125/APAN.35.7.
Elvidge, C.D., Zhizhin, M., Hsu, F.-C., Baugh, K., 2013b. VIIRS Nightfire: satellite pyrometry at night. Remote Sens. 5:4423–4449. http://dx.doi.org/10.3390/rs5094423.
Elvidge, C.D., Hsu, F.-C., Baugh, K., Ghosh, T., 2014. National trends in satellite-observed lighting: 1992–2009. In: Weng, Q. (Ed.), Global Urban Monitoring and Assessment Through Earth Observation. Boca Raton, pp. 97–120.
Elvidge, C.D., Zhizhin, M., Baugh, K., Hsu, F.-C., Ghosh, T., 2015. Methods for global survey of natural gas flaring from visible infrared imaging radiometer suite data. Energy 9: 1–16. http://dx.doi.org/10.3390/en9010014.
Falchi, F., Cinzano, P., Duriscoe, D., Kyba, C.C.M., Elvidge, C.D., Baugh, K., Portnov, B.A., Rybnikova, N.A., Furgoni, R., 2016. The new world atlas of artificial night sky brightness. Sci. Adv. 1–26. http://dx.doi.org/10.1126/sciadv.1600377.
Fan, J., Ma, T., Zhou, C., Zhou, Y., Xu, T., 2014. Comparative estimation of urban development in China's cities using socioeconomic and DMSP/OLS night light data. Remote Sens. 6:7840–7856. http://dx.doi.org/10.3390/rs6087840.
Filho, C.R.D.S., Zullo Jr., J., Elvidge, C.D., 2004. Brazil's 2001 energy crisis monitored from space. Int. J. Remote Sens. 25:2475–2482. http://dx.doi.org/10.1080/01431160410001662220.
Food and Agricultural Organization (FAO), 2015. Global Administrative Unit Layers (GAUL) Dataset, Implemented by FAO Within the CountrySTAT and Agricultural Market Information System (AMIS) Projects. URL. http://www.fao.org/geonetwork/srv/en/metadata.show?id=12691 (accessed 7.2.16).
Forbes, D.J., 2013. Multi-scale analysis of the relationship between economic statistics and DMSP-OLS night light images. GIScience & Remote Sens. 50 (5), 483–499.
Frolking, S., Milliman, T., Seto, K.C., Friedl, M.A., 2013. A global fingerprint of macro-scale changes in urban structure from 1999 to 2009. Environ. Res. Lett. 8:024004. http://dx.doi.org/10.1088/1748-9326/8/2/024004.
Gao, B., Huang, Q., He, C., Ma, Q., 2015. Dynamics of urbanization levels in China from 1992 to 2012: perspective from DMSP/OLS nighttime light data. Remote Sens. 7: 1721–1735. http://dx.doi.org/10.3390/rs70201721.
Gaston, K.J., Duffy, J.P., Bennie, J., 2015. Quantifying the erosion of natural darkness in the global protected area system. Conserv. Biol. 29:1132–1141. http://dx.doi.org/10.1111/cobi.12462.
Geldmann, J., Joppa, L.N., Burgess, N.D., 2014. Mapping change in human pressure globally on land and within protected areas. Conserv. Biol. 28 (6), 1604–1616.
Gennaioli, N., La Porta, R., De Silanes, F.L., Shleifer, A., 2014. Growth in regions. J. Econ. Growth 19 (3), 259–309.
Gleason, C.J., Hamdan, A.N., 2015. Crossing the (Watershed) Divide: Satellite Data and the Changing Politics of International River Basins. http://dx.doi.org/10.1111/geoj.12155.
Graham, S., Marvin, S., 2001. Splintering Urbanism: Networked Infrastructures, Technological Mobilities and the Urban Condition. Psychology Press, New York.
Hara, M., Okada, S., Yagi, H., Moriyama, T., Shigehara, K., Sugimori, Y., 2010. Progress for stable artificial lights distribution extraction accuracy and estimation of electric power consumption by means of DMSP/OLS nighttime imagery. Int. J. Remote Sens. Earth Sci. 1, 31–42.
He, C., Li, J., Chen, J., Shi, P., Chen, J., Pan, Y., Li, J., Zhuo, L., Toshiaki, I., 2006. The urbanization process of Bohai rim in the 1990s by using DMSP/OLS data. J. Geogr. Sci. 16: 174–182. http://dx.doi.org/10.1007/s11442-006-0205-0.
He, C., Ma, Q., Li, T., Yang, Y., Liu, Z., 2012. Spatiotemporal dynamics of electric power consumption in Chinese mainland from 1995 to 2008 modeled using DMSP/OLS stable nighttime lights data. J. Geogr. Sci. 22:125–136. http://dx.doi.org/10.1007/s11442-012-0916-3.
Henderson, M., Yeh, E.T., Gong, P., Elvidge, C., Baugh, K., 2003. Validation of urban boundaries derived from global night-time satellite imagery. Int. J. Remote Sens. 24: 595–609. http://dx.doi.org/10.1080/01431160304982.
Henderson, J.V., Storeygard, A., Weil, D.N., 2012. Measuring economic growth from outer space. Am. Econ. Rev. 102:994–1028. http://dx.doi.org/10.1257/aer.102.2.994.
Hilaire, E., 2016, Nov. 30. Inner Mongolia's Unauthorised Steel Factories - In Pictures. The Guardian, URL. https://www.theguardian.com/environment/gallery/2016/nov/30/inner-mongolia-china-unauthorised-steel-factories-in-pictures Accessed.
Hillger, D., Kopp, T., Lee, T., Lindsey, D., Seaman, C., Miller, S., Solbrig, J., Kidder, S., Bachmeier, S., Jasmin, T., Rink, T., 2013. First-light imagery from Suomi NPP VIIRS. Bull. Am. Meteorol. Soc. 94:1019–1029. http://dx.doi.org/10.1175/BAMS-D-12-00097.1.
Hodler, R., Raschky, P., 2014. Regional favoritism. Quarterly J. Econ 129, 995–1033.
Hsu, F.-C., Baugh, K., Ghosh, T., Zhizhin, M., Elvidge, C., 2015. DMSP-OLS radiance calibrated nighttime lights time series with intercalibration. Remote Sens. 7:1855–1876. http://dx.doi.org/10.3390/rs70201855.
Huang, Q., Yang, X., Gao, B., Yang, Y., Zhao, Y., 2014. Application of DMSP/OLS nighttime light images: a meta-analysis and a systematic literature review. Remote Sens. 6: 6844–6866. http://dx.doi.org/10.3390/rs6086844.
Imhoff, M.L., Lawrence, W.T., Stutzer, D.C., Elvidge, C.D., 1997. A technique for using composite DMSP/OLS "city lights" satellite data to map urban area. Remote Sens. Environ. 61:361–370. http://dx.doi.org/10.1016/S0034-4257(97)00046-1.
Jean, N., Burke, M., Xie, M., Davis, W.M., Lobell, D.B., Ermon, S., 2016. Combining satellite imagery and machine learning to predict poverty. Science 353:790–794. http://dx.doi.org/10.1126/science.aaf7894.
Jiang, L., Deng, X., Seto, K.C., 2012. Multi-level modeling of urban expansion and cultivated land conversion for urban hotspot counties in China. Landsc. Urban Plan. 108 (2), 131–139.

Katz, Y., Levin, N., 2016. Quantifying urban light pollution — a comparison between field measurements and EROS-B imagery. Remote Sens. Environ. 177:65–77. http://dx.doi.org/10.1016/j.rse.2016.02.017.

Keola, S., Andersson, M., Hall, O., 2015. Monitoring economic development from space: using nighttime light and land cover data to measure economic growth. World Dev. 66:322–334. http://dx.doi.org/10.1016/j.worlddev.2014.08.017.

Khanna, P., 2016. Connectography: Mapping the Future of Global Civilization. Random House, New York.

Kohiyama, M., Hayashi, H., Maki, N., Higashida, M., Kroehl, H.W., Elvidge, C.D., Hobson, V.R., 2004. Early damaged area estimation system using DMSP-OLS night-time imagery. Int. J. Remote Sens. 25:2015–2036. http://dx.doi.org/10.1080/01431160310001595033.

Kotavaara, O., Antikainen, H., Rusanen, J., 2011. Population change and accessibility by road and rail networks: GIS and statistical approach to Finland 1970–2007. J. Transp. Geogr. 19:926–935. http://dx.doi.org/10.1016/j.jtrangeo.2010.10.013.

Kramer, H., 1994. Observation of the Earth and Its Environment: Survey of Missions and Sensors. second ed. Verlag, Berlin/New York.

Kyba, C.M., Wagner, J.M., Kuechly, H.U., Walker, C.E., Elvidge, C.D., Falchi, F., Ruhtz, T., Fischer, J., Hölker, F., 2013. Citizen science provides valuable data for monitoring global night sky luminance. Sci. Report. 3:1835. http://dx.doi.org/10.1038/srep01835.

Kyba, C.M., Garz, S., Kuechly, H., de Miguel, A., Zamorano, J., Fischer, J., Hölker, F., 2015. High-resolution imagery of earth at night: new sources, opportunities and challenges. Remote Sens. 7:1–23. http://dx.doi.org/10.3390/rs70100001.

Lee, T.E., Miller, S.D., Turk, F.J., Schueler, C., Julian, R., Deyo, S., Dills, P., Wang, S., 2006. The NPOESS VIIRS Day/Night visible sensor. Bull. Am. Meteorol. Soc. 87:191–199. http://dx.doi.org/10.1175/BAMS-87-2-191.

Lees, L., 2002. Rematerializing geography: the "new" urban geography. Prog. Hum. Geogr. 26:101–112. http://dx.doi.org/10.1191/0309132502ph358pr.

Letu, H., Hara, M., Yagi, H., Naoki, K., Tana, G., Nishio, F., Shuhei, O., 2010. Estimating energy consumption from night-time DMPS/OLS imagery after correcting for saturation effects. Int. J. Remote Sens. 31:4443–4458. http://dx.doi.org/10.1080/01431160903277464.

Letu, H., Hara, M., Tana, G., Nishio, F., 2012. A saturated light correction method for DMSP/OLS nighttime satellite imagery. IEEE Trans. Geosci. Remote Sens. 50:389–396. http://dx.doi.org/10.1109/TGRS.2011.2178031.

Letu, H., Hara, M., Tana, G., Bao, Y., Nishio, F., 2015. Generating the nighttime light of the human settlements by identifying periodic components from DMSP/OLS satellite imagery. Environ. Sci. Technol. 49:10503–10509. http://dx.doi.org/10.1021/acs.est.5b02471.

Levin, N., Duke, Y., 2012. High spatial resolution night-time light images for demographic and socio-economic studies. Remote Sens. Environ. 119:1–10. http://dx.doi.org/10.1016/j.rse.2011.12.005.

Levin, N., Phinn, S., 2016. Illuminating the capabilities of Landsat 8 for mapping night lights. Remote Sens. Environ. 182:27–38. http://dx.doi.org/10.1016/j.rse.2016.04.021.

Li, X., Zhang, R., Huang, C., Li, D., 2015. Detecting 2014 northern Iraq insurgency using night-time light imagery. Int. J. Remote Sens. 36:3446–3458. http://dx.doi.org/10.1080/01431161.2015.1059968.

Li, X., Li, D., 2014. Can night-time light images play a role in evaluating the Syrian Crisis? Int. J. Remote Sens. 35:6648–6661. http://dx.doi.org/10.1080/01431161.2014.971469.

Li, X., Ge, L., Chen, X., 2013a. Detecting Zimbabwe's decadal economic decline using night-time light imagery. Remote Sens. 5:4551–4570. http://dx.doi.org/10.3390/rs5094551.

Li, X., Chen, F., Chen, X., 2013b. Satellite-observed nighttime light variation as evidence for global armed conflicts. IEEE J. Seletect Topics in Applied Earth Observations and Remote Sens. 6, 2302–2315.

Li, X., Xu, H., Chen, X., Li, C., 2013c. Potential of NPP-VIIRS nighttime light imagery for modeling the regional economy of China. Remote Sens. 5 (6), 3057–3081.

Liang, H., Tanikawa, H., Matsuno, Y., Dong, L., 2014. Modeling in-use steel stock in China's buildings and civil engineering infrastructure using time-series of DMSP/OLS nighttime lights. Remote Sens. 6:4780–4800. http://dx.doi.org/10.3390/rs6064780.

Liu, Zhifeng, He, Chunyang, Yang, Yang, 2011. Mapping urban areas by performing systematic correction for DMSP/OLS Nighttime Lights Time Series in China from 1992 to 2008. Geoscience and Remote Sensing Symposium (IGARSS). IEEE International, pp. 1858–1861 (IEEE, 2011).

Liu, Z., He, C., Zhang, Q., Huang, Q., Yang, Y., 2012. Extracting the dynamics of urban expansion in China using DMSP-OLS nighttime light data from 1992 to 2008. Landsc. Urban Plan. 106:62–72. http://dx.doi.org/10.1016/j.landurbplan.2012.02.013.

Liu, Q., Yang, Y., Tian, H., Zhang, B., Gu, L., 2014. Assessment of human impacts on vegetation in built-up areas in China based on AVHRR, MODIS and DMSP-OLS nighttime light data, 1992–2010. Chin. Geogr. Sci. 24:231–244. http://dx.doi.org/10.1007/s11769-013-0645-2.

Liu, Y., Wang, Y., Peng, J., Du, Y., Liu, X., Li, S., Zhang, D., 2015a. Correlations between urbanization and vegetation degradation across the world's metropolises using DMSP/OLS nighttime light data. Remote Sens. 7:2067–2088. http://dx.doi.org/10.3390/rs70202067.

Liu, Y., Saitoh, S.-I., Hirawake, T., Igarashi, H., Ishikawa, Y., 2015b. Detection of squid and Pacific saury fishing vessels around Japan using VIIRS Day/Night Band data. Proc. Asia-Pacific Adv. Netw. 39:28–39. http://dx.doi.org/10.7125/APAN.39.

Lo, C.P., 2002. Urban indicators of China from radiance-calibrated digital DMSP-OLS nighttime images. Ann. Assoc. Am. Geogr. 92:225–240. http://dx.doi.org/10.1111/1467-8306.00288.

Ma, T., Zhou, C., Pei, T., Haynie, S., Fan, J., 2012. Quantitative estimation of urbanization dynamics using time series of DMSP/OLS nighttime light data: a comparative case study from China's cities. Remote Sens. Environ. 124:99–107. http://dx.doi.org/10.1016/j.rse.2012.04.018.

Ma, T., Zhou, Y., Wang, Y., Zhou, C., Haynie, S., Xu, T., 2014a. Diverse relationships between Suomi-NPP VIIRS night-time light and multi-scale socioeconomic activity. Remote Sens. Lett. 5:652–661. http://dx.doi.org/10.1080/2150704X.2014.953263.

Ma, L., Wu, J., Li, W., Peng, J., Liu, H., 2014b. Evaluating saturation correction methods for DMSP/OLS nighttime light data: a case study from China's cities. Remote Sens. 6:9853–9872. http://dx.doi.org/10.3390/rs6109853.

Ma, T., Zhou, C., Pei, T., Haynie, S., Fan, J., 2014c. Responses of Suomi-NPP VIIRS-derived nighttime lights to socioeconomic activity in China's cities. Remote Sens. Lett. 5:165–174. http://dx.doi.org/10.1080/2150704X.2014.890758.

Mellander, C., Lobo, J., Stolarick, K., Matheson, Z., 2015. Night-time light data: a good proxy measure for economic activity? PloS one 10 (10), e0139779.

Michalopoulos, S., Papaioannou, E., 2013. Pre-Colonial Ethnic Institutions and Contemporary African Development. Econometrica 81 (1), 113–152.

Michalopoulos, S., Papaioannou, E., 2014. National institutions and subnational development in Africa. Q. J. Econ. 129 (1), 151–213.

Miller, S.D., Mills, S.P., Elvidge, C.D., Lindsey, D.T., Lee, T.F., Hawkins, J.D., 2012. Suomi satellite brings to light a unique frontier of nighttime environmental sensing capabilities. Proc. Natl. Acad. Sci. 109:15706–15711. http://dx.doi.org/10.1073/pnas.1207034109.

Miller, S.D., Straka, W., Mills, S.P., Elvidge, C.D., Lee, T.F., Solbrig, J., Walther, A., Heidinger, A.K., Weiss, S.C., 2013. Illuminating the capabilities of the Suomi National Polar-orbiting Partnership (NPP) visible infrared imaging radiometer suite (VIIRS) day/night band. Remote Sens. 5:6717–6766. http://dx.doi.org/10.3390/rs5126717.

Mills, S., Weiss, S., Liang, C., 2013. VIIRS day/night band (DNB) stray light characterization and correction. Proc. SPIE 8866. http://dx.doi.org/10.1117/12.2023107.

Min, B., Gaba, K., 2014. Tracking electrification in Vietnam using nighttime lights. Remote Sens. 6:9511–9529. http://dx.doi.org/10.3390/rs6109511.

Min, B., Gaba, K.M., Sarr, O.F., Agalassou, A., 2013. Detection of rural electrification in Africa using DMSP-OLS night lights imagery. Int. J. Remote Sens. 34:8118–8141. http://dx.doi.org/10.1080/01431161.2013.833358.

Molthan, A., Jedlovec, G., 2013. Satellite observations monitor outages from superstorm Sandy. EOS Trans. Am. Geophys. Union 94:53–54. http://dx.doi.org/10.1002/2013EO050001.

NOAA/NGDC, 2017a. Data Services/Pricing. [WWW Document]. URL https://www.ngdc.noaa.gov/eog/services.html (accessed 1.31.17).

NOAA/NGDC, 2017b. VIIRS DNB Cloud Free Composites: Version 1 Nighttime VIIRS Day/Night Band Composites [WWW Document]. URL http://ngdc.noaa.gov/eog/viirs/download_monthly.html (accessed 1.31.17).

Nordhaus, W., Chen, X., 2015. A sharper image? Estimates of the precision of nighttime lights as a proxy for economic statistics. J. Econ. Geogr. 15:217–246. http://dx.doi.org/10.1093/jeg/lbu010.

Ou, J., Liu, X., Li, X., Li, M., Li, W., 2015. Evaluation of NPP-VIIRS nighttime light data for mapping global fossil fuel combustion CO_2 emissions: a comparison with DMSP-OLS nighttime light data. PLoS One http://dx.doi.org/10.1371/journal.pone.0138310.

Pandey, B., Joshi, P.K., Seto, K.C., 2013. Monitoring urbanization dynamics in India using DMSP/OLS night time lights and SPOT-VGT data. Int. J. Appl. Earth Obs. Geoinf. 23:49–61. http://dx.doi.org/10.1016/j.jag.2012.11.005.

Panifilova, E.A., 2016. Corruption indices for Russian Regions. In: Shacklock, A., Galtung, F. (Eds.), Measuring Corruption. Routledge, London and New York, pp. 189–203.

Parés-Ramos, I.K., Álvarez-Berríos, N.L., Aide, T.M., 2013. Mapping urbanization dynamics in major cities of Colombia, Ecuador, Perú, and Bolivia using night-time satellite imagery. Land 2 (1), 37–59.

Pinkovskiy, M.L., 2013. Economic Discontinuities at Borders: Evidence From Satellite Data on Lights at Night. MA, Cambridge.

Raupach, M.R., Rayner, P.J., Paget, M., 2010. Regional variations in spatial structure of nightlights, population density and fossil-fuel CO_2 emissions. Energ Policy 38:4756–4764. http://dx.doi.org/10.1016/j.enpol.2009.08.021.

RIA Novosti, 2012, 28 Feb. Где в России добывают нефть – рейтинг регионов [Where in Russia Produces Oil - Ratings of Regions]. URL https://ria.ru/research_rating/20120228/578638606.html (accessed 12.19.16).

Rohner, D., Thoenig, M., Zilibotti, F., 2013. Seeds of distrust: conflict in Uganda. J. Econ. Growth 18:217–252. http://dx.doi.org/10.1007/s10887-013-9093-1.

Román, M.O., Stokes, E.C., 2014. Holidays in lights: tracking cultural patterns in demand for energy services. Earth's Future 3:182–205. http://dx.doi.org/10.1002/2014EF000285.

Seaman, C.J., Miller, S.D., 2015. A dynamic scaling algorithm for the optimized digital display of VIIRS Day/Night Band imagery. Int. J. Remote Sens. 36:1839–1854. http://dx.doi.org/10.1080/01431161.2015.1029100.

Shao, X., Cao, C., Zhang, B., Qiu, S., Elvidge, C., Von Hendy, M., 2014. Radiometric Calibration of DMSP-OLS Sensor Using VIIRS Day/Night Band 9264, 92640A1–92640A8. http://dx.doi.org/10.1117/12.2068999.

Shi, K., Chang, H., Bailang, Y., Bing, Y., Yixiu, H., Jianping, W., 2014. Evaluation of NPP-VIIRS night-time light composite data for extracting built-up urban areas. Remote Sens. Lett. 5:358–366. http://dx.doi.org/10.1080/2150704x.2014.905728.

Shi, K., Yu, B., Hu, Y., Huang, C., Chen, Y., Huang, Y., Chen, Z., Wu, J., 2015. Modeling and mapping total freight traffic in China using NPP-VIIRS nighttime light composite data. GIScience Remote Sens. 52:274–289. http://dx.doi.org/10.1080/15481603.2015.1022420.

Small, C., Elvidge, C.D., 2013. Night on earth: mapping decadal changes of anthropogenic night light in Asia. Int. J. Appl. Earth Obs. Geoinf. 22:40–52. http://dx.doi.org/10.1016/j.jag.2012.02.009.

Small, C., Sousa, D., 2016. Humans on Earth; Global Extents of Anthropogenic Land Cover from Remote Sensing. Anthropocene. http://dx.doi.org/10.1016/j.ancene.2016.04.003.

Small, C., Pozzi, F., Elvidge, C., 2005. Spatial analysis of global urban extent from DMSP-OLS night lights. Remote Sens. Environ. 96:277–291. http://dx.doi.org/10.1016/j.rse.2005.02.002.

Small, C., Elvidge, C.D., Balk, D., Montgomery, M., 2011. Spatial scaling of stable night lights. Remote Sens. Environ. 115:269–280. http://dx.doi.org/10.1016/j.rse.2010.08.021.

Small, C., Elvidge, C.D., Baugh, K., 2013. Mapping urban structure and spatial connectivity with VIIRS and OLS night light imagery. Jt. Urban Remote Sens. Event 2013 (856): 230–233. http://dx.doi.org/10.1109/JURSE#.2013.6550707.
Stern, P., 1993. A second environmental science: human-environment interactions. Science 260, 1897–1899.
Stevens, F.R., Gaughan, A.E., Linard, C., Tatem, A.J., 2015. Disaggregating census data for population mapping using random forests with remotely-sensed and ancillary data. PLoS One 10, e0107042. http://dx.doi.org/10.1371/journal.pone.0107042.
Straka, W., Seaman, C., Baugh, K., Cole, K., Stevens, E., Miller, S., 2015. Utilization of the Suomi National Polar-orbiting Partnership (NPP) Visible Infrared Imaging Radiometer Suite (VIIRS) Day/Night Band for Arctic ship tracking and fisheries management. Remote Sens. 7:971–989. http://dx.doi.org/10.3390/rs70100971.
Su, Y., Chen, X., Wang, C., Zhang, H., Liao, J., Ye, Y., Wang, C., 2015. A new method for extracting built-up urban areas using DMSP-OLS nighttime stable lights: A case study in the Pearl River Delta, southern China. GIScience & Remote Sens. 52 (2), 218–238.
Sullivan III, W.T., 1989. A 10 km resolution image of the entire night-time Earth based on cloud-free satellite photographs in the 400–1100 nm band. Remote Sens. 10 (1), 1–5.
Sutton, P., 1997. Modeling population density with night-time satellite imagery and GIS. Comput. Environ. Urban. Syst. 21:227–244. http://dx.doi.org/10.1016/S0198-9715(97)01005-3.
Sutton, P., Costanza, R., 2002. Global estimates of market and non-market values derived from nighttime satellite imagery, land cover, and ecosystem service valuation. Ecol. Econ. 41:509–527. http://dx.doi.org/10.1016/S0921-8009(02)00097-6.
Sutton, P., Roberts, D., Elvidge, C., Baugh, K., 2001. Census from heaven: an estimate of the global human population using night-time satellite imagery. Int. J. Remote Sens. 22: 3061–3076. http://dx.doi.org/10.1080/01431160010007015.
Sutton, P., Elvidge, C., Ghosh, T., 2007. Estimation of gross domestic product at sub-national scales using nighttime satellite imagery. Int. J. Ecol. Econ. Stat. 8, 5–21.
Tan, M., 2015. Urban growth and rural transition in China based on DMSP/OLS nighttime light data. Sustainability 7, 8768–8781.
Tanaka, K., Keola, S., 2016. Shedding light on the shadow economy: a nighttime light approach. J. Dev. Stud. http://dx.doi.org/10.1080/00220388.2016.1171845.
Tian, J., Zhao, N., Samson, E.L., Wang, S., 2014. Brightness of nighttime lights as a proxy for freight traffic. A Case Study of China 7, 206–212.
Tibbetts, J., 2002. Coastal cities: living on the edge. Environ. Health Perspect. 110: 674–681. http://dx.doi.org/10.1289/ehp.110-a674.
Tobler, W., 1969. Confirmation of settlement size coefficients. Area 1, 30–34.
Townsend, A.C., Bruce, D., 2010. The use of night-time lights satellite imagery as a measure of Australia's regional electricity consumption and population distribution. Int. J. Remote Sens. 31:4459–4480. http://dx.doi.org/10.1080/01431160903261005.
Venter, O., Sanderson, E.W., Magrach, A., Allan, J.R., Beher, J., Jones, K.R., Possingham, H.P., Laurence, W.F., Wood, P., Fekete, B.M., Levy, M.A., Watson, J.E., 2016. Sixteen years of change in the global terrestrial human footprint and implications for biodiversity conservation. Nat. Commun. 7. http://dx.doi.org/10.1038/ncomms12558.
Weidmann, N.B., Schutte, S., 2016. Using night light emissions for the prediction of local wealth. J. Peace Res. 0022343316630359. http://dx.doi.org/10.1177/0022343316630359.
Welch, R., 1980. Monitoring urban population and energy utilization patterns from satellite data. Remote Sens. Environ. 9:1–9. http://dx.doi.org/10.1016/0034-4257(80)90043-7.
Witmer, F.D.W., O'Loughlin, J., 2011. Detecting the effects of wars in the Caucasus regions of Russia and Georgia using radiometrically normalized DMSP-OLS nighttime lights imagery. GIScience Remote Sens. 48:478–500. http://dx.doi.org/10.2747/1548-1603.48.4.478.
World Bank, 2011. Global Gas Flaring Reduction Partnership (GGFR): Improving Energy Efficiency and Mitigating Impact on Climate Change.
Xiao, P.F., Wang, X.H., Feng, X.Z., Zhang, X.L., Yang, Y.K., 2014. Detecting China's urban expansion over the past three decades using nighttime light data. IEEE J. Sel. Top. Appl. Earth Obs. Remote Sens. 7:4095–4106. http://dx.doi.org/10.1109/Jstars.2014.2302855.
Xie, Y., Weng, Q., Weng, A., Xie, Y., Weng, Q., Weng, A., 2014. A Comparative Study of NPP-VIIRS and DMSP-OLS Nighttime Light Imagery for Derivation of Urban Demographic Metrics. 2014 3rd Intl. Workshop on Earth Obs. Remote Sens. Applications. http://dx.doi.org/10.1109/EORSA.2014.6927907.
Xu, T., Ma, T., Zhou, C., Zhou, Y., 2014. Characterizing spatio-tempral dynamics of urbanization in China using time series of DMSP/OLS nightl ight data. Remote Sens. 6: 7708–7731. http://dx.doi.org/10.3390/rs6087708.
Xu, H., Yang, H., Li, X., Jin, H., Li, D., 2015. Multi-scale measurement of regional inequality in mainland China during 2005–2010 using DMSP/OLS night light imagery and population density grid data. Sustainability 7:13469–13499. http://dx.doi.org/10.3390/su71013469.
Yi, Kunpeng, Tani, Hiroshi, Li, Qiang, Zhang, Jiquan, Guo, Meng, Bao, Yulong, Wang, Xiufeng, Li, Jing, 2014. Mapping and evaluating the urbanization process in northeast China using DMSP/OLS nighttime light data. Sensors 14 (2), 3207–3226.
Zhang, Q., Seto, K.C., 2011. Mapping urbanization dynamics at regional and global scales using multi-temporal DMSP/OLS nighttime light data. Remote Sens. Environ. 115: 2320–2329. http://dx.doi.org/10.1016/j.rse.2011.04.032.
Zhang, Q., Seto, K., 2013. Can night-time light data identify typologies of urbanization? A global assesment of success and failures. Remote Sens. 5:3476–3494. http://dx.doi.org/10.3390/rs5073476.
Zhang, Q., He, C., Liu, Z., 2014. Studying urban development and change in the contiguous United States using two scaled measures derived from nighttime lights data and population census. GIScience & Remote Sens. 51 (1), 63–82.
Zhao, M., Cheng, W., Liu, Q., Wang, N., 2016. Spatiotemporal measurement of urbanization levels based on multiscale units: A case study of the Bohai Rim Region in China. J. Geogr. Sci. 26 (5), 531–548.
Zhou, Y., Smith, S.J., Elvidge, C.D., Zhao, K., Thomson, A., Imhoff, M., 2014. A cluster-based method to map urban area from DMSP/OLS nightlights. Remote Sens. Environ. 147, 173–185.
Zhou, Y., Ma, T., Zhou, C., Xu, T., 2015a. Nighttime light derived assessment of regional inequality of socioeconomic development in China. Remote Sens. 7:1242–1262. http://dx.doi.org/10.3390/rs70201242.
Zhou, N., Hubacek, K., Roberts, M., 2015b. Analysis of spatial patterns of urban growth across South Asia using DMSP-OLS nighttime lights data. Appl. Geogr. 63:292–303. http://dx.doi.org/10.1016/j.apgeog.2015.06.016.
Zhou, L., Divakarla, M., Liu, X., 2016. An overview of the Joint Polar Satellite System (JPSS) science data product calibration and validation. Remote Sens. 8:139. http://dx.doi.org/10.3390/rs8020139.
Zhuo, L., Ichinose, T., Zheng, J., Chen, J., Shi, P.J., Li, X., 2009. Modelling the population density of China at the pixel level based on DMSP/OLS non-radiance-calibrated night-time light images. Int. J. Remote Sens. 30:1003–1018. http://dx.doi.org/10.1080/01431160802430693.
Ziskin, D., Baugh, K., Hsu, F.C., Elvidge, C.D., 2010. Methods used for the 2006 radiance lights. Proc. Asia-Pacific Advanced Network 30:131–142. http://dx.doi.org/10.7125/APAN.30.18.